

Tectonic characterization of the cataclastic structures in the
crystalline Precambrian rocks of the Sindhudurg District,

Southern Maharashtra

A Dissertation Report for

GEO - 651 Dissertation

Credits: 16

Submitted in partial fulfillment of Master's Degree

Msc. Applied Geology

by

YADHANESH VAZARKAR

22P045027

61211802929

201900978

Under the Supervision of

DR. NICOLE SEQUEIRA

School of Earth, Ocean and Atmospheric Science,

Applied Geology



Goa University

May 2024



Seal of the School

Examined by:

DECLARATION BY STUDENT

I hereby declare that the data presented in this Dissertation report entitled 'Tectonic characterization of the cataclastic structures in the crystalline Precambrian rocks of the Sindhudurg District, Southern Maharashtra' is based on the results of investigations carried out by me in M.Sc. Applied Geology at the School of Earth, Ocean and Atmospheric Science, Goa University under the supervision of Dr. Nicole Sequeira and the same has not been submitted elsewhere for the award of a degree or diploma by me. Further, I understand that Goa University or its authorities will not be responsible for the correctness of observations / experimental or other findings given the dissertation.

I hereby authorize the University authorities to upload this dissertation to the dissertation repository or anywhere else as the UGC regulations demand and make it available to anyone as needed.

Yadhanesh Vazarkar

22P0450027

M.Sc. Applied Geology

School of Earth, Ocean and Atmospheric Sciences

Date: 2/5/24

Place: Goa University

COMPLETION CERTIFICATE

This is to certify that the dissertation report Tectonic characterization of the cataclastic structures in the crystalline Precambrian rocks of the Sindhudurg District, Southern Maharashtra is a bonafide work carried out by **Mr. Yadhanesh Vazarkar** under my supervision in partial fulfillment of the requirements for the award of the degree of M.Sc. in the Discipline Applied Geology at the School of Earth, Ocean and Atmospheric Science, Goa University.



Dr. Nicole Sequeira
Assistant Professor
Goa University

Date: 02.05.2024



Senior Prof. Sanjeev Ghadi

Dean, School of Earth, Ocean and Atmospheric Sciences

Goa University

Date:

Place: Goa University



School stamp

Tectonic characterization of the cataclastic structures
in the crystalline Precambrian rocks of the Sindhudurg District,

Southern Maharashtra

A Dissertation Report for

GEO - 651 Dissertation

Credits: 16

Submitted in partial fulfillment of Degree M.Sc. Applied Geology

by

Yadhanesh Vazarkar

Roll Number: 22P045027

ABC ID-61211802929

PRN 201900978

Under the Supervision of

DR. NICOLE SEQUEIRA

School of Earth, Ocean and Atmospheric Science,

Applied Geology



Goa University

May 2024

Examined by:

Seal of the School

DECLARATION BY STUDENT

I hereby declare that the data presented in this Dissertation report entitled ‘Tectonic characterization of the cataclastic structures in the crystalline Precambrian rocks of the Sindhudurg District, Southern Maharashtra’ is based on the results of investigations carried out by me in M.Sc. Applied Geology at the School of Earth, Ocean and Atmospheric Science, Goa University under the supervision of Dr. Nicole Sequeira and the same has not been submitted elsewhere for the award of a degree or diploma by me. Further, I understand that Goa University or its authorities will not be responsible for the correctness of observations / experimental or other findings given the dissertation.

I hereby authorize the University authorities to upload this dissertation to the dissertation repository or anywhere else as the UGC regulations demand and make it available to anyone as needed.

Yadhanesh Vazarkar

22P0450027

M.Sc. Applied Geology

School of Earth, Ocean and Atmospheric Sciences

Date:

Place: Goa University

COMPLETION CERTIFICATE

This is to certify that the dissertation report Tectonic characterization of the cataclastic structures in the crystalline Precambrian rocks of the Sindhudurg District, Southern Maharashtra is a bonafide work carried out by **Mr. Yadhanesh Vazarkar** under my supervision in partial fulfillment of the requirements for the award of the degree of M.Sc. in the Discipline Applied Geology at the School of Earth, Ocean and Atmospheric Science, Goa University.

Date:

Dr. Nicole Sequeira
Assistant Professor
Goa University

Senior Prof. Sanjeev Ghadi

School stamp

Dean, School of Earth, Ocean and Atmospheric Sciences

Goa University

Date:

Place: Goa University

ACKNOWLEDGEMENT

I am immensely grateful to Dr. Nicole Sequeira, whose pivotal role in my thesis made this achievement possible. Dr. Sequeira not only served as an exceptional supervisor but also acted as a mentor, offering invaluable support and guidance throughout my research journey. Her profound expertise and insights significantly shaped my study and deepened my understanding of the subject matter. Additionally, Mr. Santra, & Mr. Vishal served as a source of inspiration I also extend my heartfelt appreciation to my classmates whose unwavering support, encouragement, and guidance were instrumental in surmounting any challenges encountered along the way. Additionally, I would like to extend my heartfelt thanks to my dear friends, Meldroy Vas and Deevyam Rawal for accompanying me during the fieldwork and offering valuable assistance throughout the journey.

I am immensely thankful to my parents for their unwavering belief in me and their steadfast support throughout my journey of completing my M.Sc. dissertation. Their encouragement and blessings have been the cornerstone of my success, without which this achievement would have been unimaginable. Additionally, I extend my heartfelt gratitude to the Applied Geology Programme at SEOAS - Goa University.. I am also indebted to the faculty members of the Programme, including Dr. Anthony A. A Viegas (Vice Dean), Dr. Niyati Kalangutkar, Dr. Poornima Sawant, Mr. Mahesh Mayekar, and Dr. Pooja Ghadi, for their unwavering assistance and support whenever I required it. Moreover, I wish to recognize the contributions of the non-teaching staff of our department, including Mrs. Sangetta Tilve, Mr. Rajesh, and Mrs. Tulsi.

INDEX

CHAPTER I : INTRODUCTION	X
Introduction	1
AIMS & OBJECTIVES	8
AREA OF STUDY	8
PHYSIOGRAPHY	9
Drainage	10
Climate	10
METHODOLOGY	11
CHAPTER II : Background Geology	13
Geological Features of Sindhudurg	13
Geology Of The Study Area	17
CHAPTER III :FIELD CHARACTERISTICS & STRUCTURES	19
CHAPTER IV:MINERAL CHEMISTRY & MICROSTRUCTURES	30
General petrology of the region.	30
Petrography of Cataclastic shears	31
CHAPTER V :THERMOBAROMETRY	50
CHAPTER VI : DISSCUSSION AND CONCLUSION.....	53
CHAPTER VII : REFERENCE	57

LIST OF FIGURES

Figure no	Description	Page no.
Table No 2.1	Lithostratigraphy of the sindhudurg district	15
Table No 4.1	Mineral chemistry and Structural Formulae of Garnet based on 12 oxygen	33
Table No 4.2	Mineral chemistry and Structural Formulae of Pyroxene based on 12 oxygen.	36
Table No 4.3	Mineral chemistry and Structural Formulae of scapolite based on 12 oxygen Table No 4.4: Mineral chemistry and Structural Formulae of Biotite based on 11 oxygen	37
Table No 4.4	Mineral chemistry and Structural Formulae of Orthoclase based on 8 oxygen	46
Table No 5.1	Table No 5.1-Temperature (°C) at 7.5kbar conditions of calcic layer using conventional thermobarometers.	50
Table No5.2	Pressure (Kbr) at 600°C conditions of calcic layer using conventional thermobarometers.	50

LIST OF FIGURES

Figure no.	Description	Page no.
Figure 1.1	Simplified diagram illustrating vertical variations in shear zones and shear zone fabrics.	3
Figure 1.2	Schematic cross section through a shear zone, showing the vertical distribution of fault-related rock	4
Figure.1.3	Drawing of the common elements within a Riedel shear system	6
Figure 1.4	Political map of Sindhudurg district Maharashtra.	9
Figure.2.1	:Generalized geological map of Pernem (Goa)-Phonda (Maharashtra) corridor adopted from Rekha and Bhattacharya (2014)	15
Figure.2.2	Generalized geological map of Pernem (Goa)-Phonda (Maharashtra) corridor adopted from Rekha and Bhattacharya (2014)	17
Figure.3.1	Lithological map of the study area showing the locations selected for detailed investigations.	20
Figure 3.2	Photographs showing cataclastic shears in biotite schists interlayered with cm thick calc-silicate layers in the field.	22
Figure 3.3	Plan view photograph of termination of cataclastic shear oriented in $N60^\circ$ within a garnet bearing biotite schist, at the contact of garnet absent schist.	23
Figure 3.4	Stereonet plots for Outcrops in the north eastern part of the study area	24
Figure 3.5-	Stereonet plots for Outcrops in the central part of the study area showing SW foliation.	25
Figure 3.6	Plan view photograph of the cataclastic shears oriented $N140^\circ$ (parallel set marked in red) & conjugate shears (marked in blue) of $N60^\circ$ & $N110^\circ$.	27
Figure 3.7	Shear senses associated with different cataclastic shears.	28

Figure 3.8 -	Orientation of shears using Rose diagram	29
Figure 4.1-	Photograph of hand specimen & thinsection showing two different lithologies	31
Figure 4.2 -	Plane polarized photomicrograph showing Garnet surrounded by Diopside and scapolite, garnets are characterizing an orientation	32
Figure 4.3-	Plane polarized photomicrograph showing Garnet surrounded by Diopside	34
Figure 4.4-	Ternary plot for Classification of pyroxenes.	35
Figure 4.5 -	Plane polarized photomicrograph showing grains of calcite and apatite surrounded by a cloudy matrix	38
Figure 4.6-	Plane polarized photomicrograph showing grains of hornblende surrounded by diopside.	39
Figure 4.7-	Plane polarized photomicrograph showing grains of diopside wrapping around skeletal garnets..	40
Figure 4.8-	Plane polarized photomicrograph of garnet in the biotite domain	41
Figure 4.9-	Cross polarized photomicrograph of Quartz showing bulging & straight grain boundaries.	44
Figure 4.10-	Tertiary plot for Feldspars.	45
Figure.4.11-	Plane polarized photomicrograph of saussuritization K feldspar along the shear	47
Figure 4.12:	BSE images showing secondary precipitation of iron oxides along the shear planes	49
Figure 4.13:	BSE images showing secondary precipitation along the shear planes	49
Figure 6.1:	Correlating oriented shears of the N-S foliated outcrop with the Riedel shear diagram.	55
Figure 6.2:	Correlating oriented shears of the ESE foliated outcrop with the Riedel shear diagram	55

ABSTRACT

The study focuses on the cataclastic shears present in the multiply deformed Precambrian garnetiferous biotite schists and amphibolites in and around Sawantwadi in the Sindhudurg district of Maharashtra, India. Few previous studies have recognized these brittle structures, labeling them as “shear fabrics” (Rekha et al., 2014) or “boxwork structures” (V. Venugopal 2023, F. Azhar 2022). The present study explores the regional and mesoscale structural characteristics, microstructures and geothermobarometry of these cataclastic shears and their host schistose rocks. The cataclastic shears appear as mm to cm-thick densely intersecting resistant planes within the schists that stand out from the country rock due to differential weathering. Two major conjugate shear sets are present in the area, with bisecting directions of ESE and NNE, which are near parallel to the foliation in the schistose rocks. Subsidiary orientations of vertical cataclastic shears are NE & E-W. These orientations can be compared to Y, P, T, R and R' brittle shears which indicate that the major stress directions during the formation of the shears was NE & ESE. Petrographic analysis indicates that the cataclastic shears are associated with brecciation, grain size reduction and rotation of garnet, plagioclase, and hornblende in the schists and of clinopyroxene, garnet, scapolite in the calcareous layers. The presence of fluids during shearing is interpreted from the occasional secondary mineral precipitation of fibrous calc-aluminosilicate minerals, epidote, chlorite, quartz, or pseudotachylite, within the fractures. The peak metamorphic temperature of deformation in the host rock was 526°C to 902°C and pressure was 5.6 kbars to 7.2 kbars before the rocks were affected by brittle deformation.

CHAPTER I : INTRODUCTION

Introduction

The earth has experienced several tectonic cycles of accretion and disassociation of tectonic plates from the time of its formation to the present day. Several supercontinents have been proposed to have existed throughout geologic time, including the Columbia Supercontinent in the Paleoproterozoic,(Rogers and Santosh, 2002) the Rodinia Supercontinent in the Late Mesoproterozoic to Neoproterozoic, (Condie, K. C. 2001) and the Gondwana Supercontinent in the late Neoproterozoic.(Rekha et al., 2014).

The Indian subcontinent comprising Archean to Proterozoic cratons, has been proposed to be a part of different Supercontinents but little clarity and agreement exists on its exact position within these Supercontinents. The Archean Dharwar Craton of South India is the most investigated craton from Peninsular India, to identify the position of the Indian landmass within Precambrian Supercontinents. The craton itself is proposed to extend into Eastern Madagascar, which has now rifted apart from the West Coast of India. The northern continuity of the Dharwar craton beneath the Cretaceous Deccan Traps has also been challenged recently by Rekha and Bhattacharya (2014)

Rifted Precambrian cratons are correlated based on the continuity of terrain boundary shear zones across continents, and on the similarity between the tectonic histories of the segments (Bhattacharya et al., 2023). Shear zones can extend from regional scale to nano scale, and are zones of high strain accumulation. Shear zones exhibit diverse

micro-scale deformation mechanisms, typically classified into plastic (or crystal-plastic) shear zones dominated by crystal-plastic mechanisms like dislocation creep and twinning, and frictional or brittle shear zones governed by brittle deformation mechanisms such as grain fracture and frictional sliding. Brittle shear zones, often referred to as faults or fault cores, are associated with seismic activity, contrasting with seismic creep observed in plastic shear zones. However, many shear zones display a combination of both plastic and brittle deformation mechanisms, leading to terms like brittle-plastic or frictional-viscous shear zones, reflecting the interplay between these processes (Rutter, 1986; Fousseis and Handy, 2008; Stipp et al., 2002).

Crystal-plasticity, influenced by factors such as mineral composition, temperature, pressure, and the presence of fluids, as well as strain rate and grain size, plays a crucial role in the development of shear zones within different rock types. Shear zones can form under various conditions, with salt forming them even in wet surface environments, marbles at deeper crustal depths, quartzites around 300 °C, and feldspathic rocks above ~450 °C. This wide temperature range highlights the transition from brittle to plastic behavior. In continental rocks rich in quartz and feldspar, this transition spans from 300 to 450 °C, characterized by fractured feldspar within a matrix of recrystallized quartz deformed by dislocation creep. Given that shear zones can traverse entire crusts and lithospheres, they exhibit a diverse range of microstructural and rheological facies at different depths. Moreover, many large high-grade crustal shear zones display evidence of subsequent reactivation through lower grade mylonitization and eventual brittle faulting during exhumation.

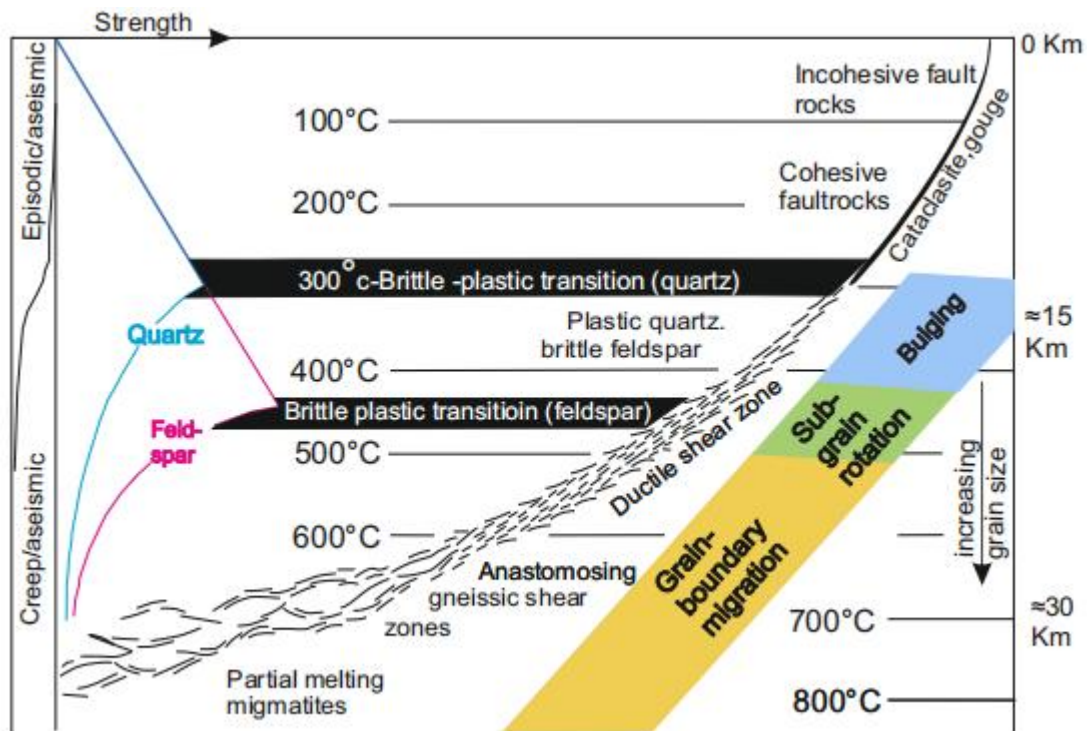


Figure 1.1- Simplified diagram illustrating vertical variations in shear zones and shear zone fabrics modified from Fossen, H., & Cavalcante (2017). The brittle-plastic transitions for quartz and feldspar and dominant recrystallization mechanisms (bulging, subgrain rotation and grain-boundary migration) are related to temperature, but also depend on strain rate and the amount of fluids present.

Classification of rocks within the shear zone

In shallower areas, faults tend to be narrower and exhibit more brittle behavior. This means they are prone to breaking and fracturing, resulting in a network of interconnected faults containing rocks that often lack cohesion, like breccia and gouge. As we go deeper, the pressure from the surrounding rocks squeezes the fault walls together, leading to more thorough and widespread deformation. This causes the rock constituents to become finer, transitioning into cataclasites and microbreccias, sometimes with the presence of pseudotachylites. Further down, the rocks develop a foliated texture, and recrystallization occurs alongside deformation, forming mylonites. As the depth increases, the width of the fault zone expands, and the deformation becomes more ductile, spreading more evenly throughout the rock matrix.

At great depths, the shear forces are distributed over a wide area, and the intensity of deformation at any single point decreases. The rocks become more ductile, and gneisses form, resembling those formed during regional orogenic metamorphism.

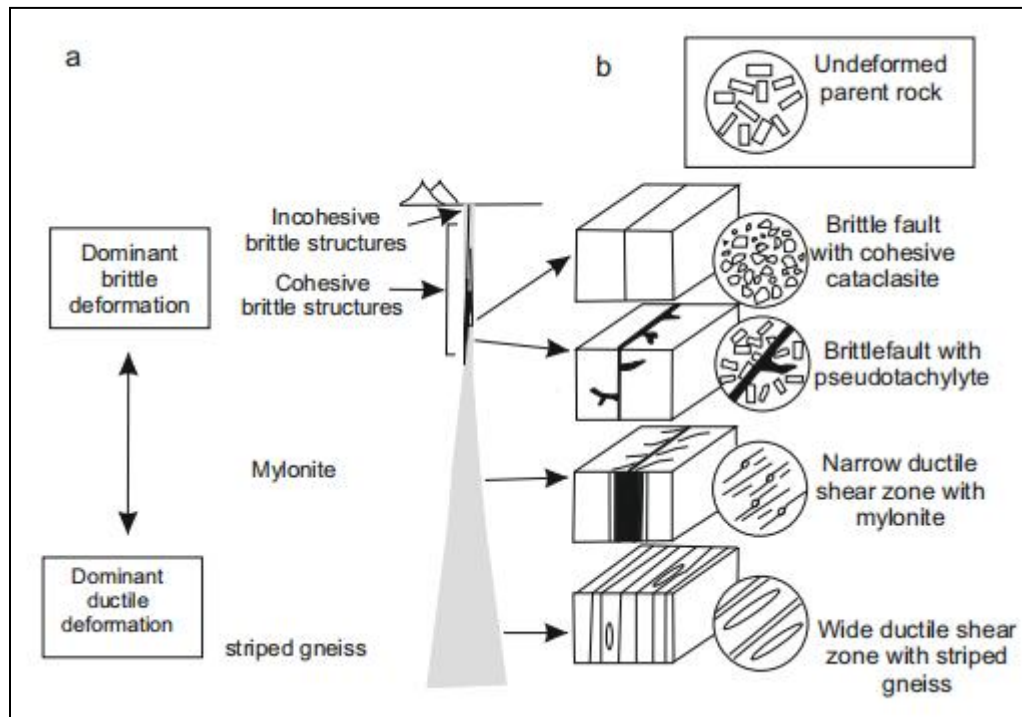


Figure 1.2-Schematic cross section through a shear zone, showing the vertical distribution of fault-related rock types, ranging from non-cohesive gouge and breccia near the surface through progressively more cohesive and foliated rocks.modified after Passchier and Trouw (1996)

Brittle deformation mechanisms dominantly include granular flow which is common during shallow deformation of porous rocks and sediments, while cataclastic flow occurs during deformation of well-consolidated rocks. Cataclastic flow involves microfracturing, frictional sliding on grain boundaries and rigid rotation of grain fragments. Microscopic evidence pointing towards cataclastic flow includes the presence of microfractures and shifts along cleavage planes, alongside the movement or rotation of solid particles without internal crystal-plastic alteration.

Cataclastic shears are narrow areas where rocks have been squeezed and broken either along fault lines or within shear zones. They show intense cracking and grinding of the rock. Secondary minerals may occur in cataclastic shears where minerals grow on the fresh surfaces formed during grain crushing or grain boundary sliding.

Another prominent brittle structure is deformation bands. These are mm- to cm-thick zones of localized compaction, shear and/or dilation in deformed rocks. The strain hardening that occurs during the growth of many deformation bands also makes them different from fractures. The physical properties of deformation bands are generally not fault-like, for the mechanism is not one of stick-slip deformation (Byerlee and Brace, 1968). Instead, the shear is accomplished through a mechanism that involves stress-induced collapse of porosity, grain-scale fracturing, grain-size reduction, and cataclastic flow (Aydin, 1978; Aydin and Johnson, 1978; Antonellini et al., 1994a,b), without development of a discrete fracture surface. Deformation bands tend to define sets with preferred orientation, for example parallel or as conjugate sets. Deformation bands emerge as crucial primary structures, laying the groundwork before the creation of substantial faults. Their presence hints at a pivotal role in the genesis of these larger faults, some spanning several tens of meters in offset.

Riedel shear structures are common fault patterns identified within shear zones and related to the embryonic stages of fault formation. Riedel shear is also used on a large-scale fault pattern and may refer to as many as five direction families of associated fractures. In that case, individual fractures remain active after the other types developed so that synchronous movement on all fractures accommodate strain in the fault zone. The geometrical arrangement of Riedel shears is indicative of the

sense of movement within the wrench zone and is therefore widely used for the interpretation of its kinematic evolution.

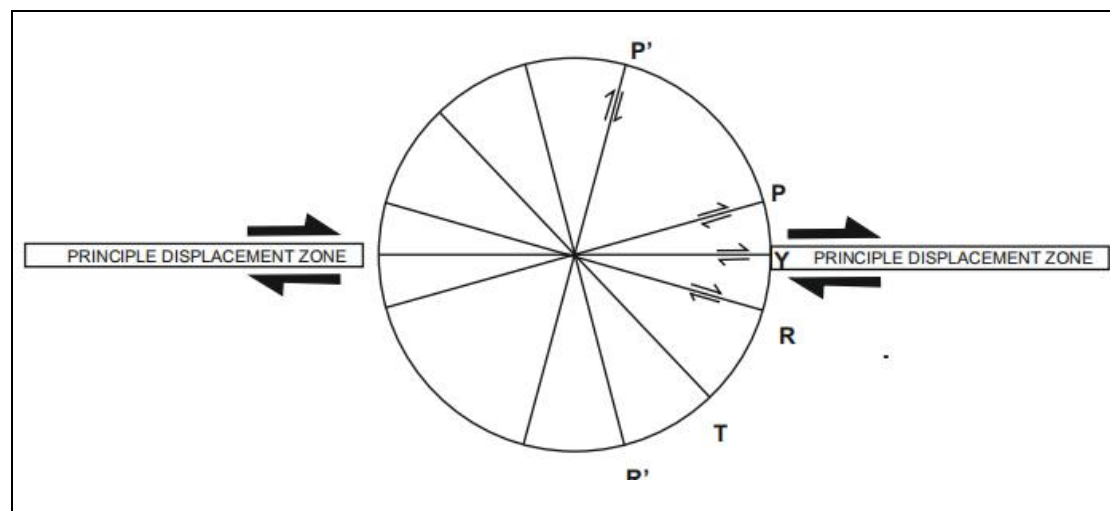


Figure.1.3-. Drawing of the common elements within a Riedel shear system, After Bartlett et al. (1981) and Woodcock and Schubert (1994).

R Riedel shears are normally the first subsidiary fractures to occur and generally build the most prominent set. They develop at an acute angle, typically 10-20° clockwise to a dextral main fault, anticlockwise to a sinistral strike-slip fault. They often form an *en échelon* and overstepping array synthetic to the main fault.

R' shears are antithetic faults oriented at a high angle approximately 75° clockwise to a dextral, anticlockwise to a sinistral main fault plane, conjugate with the R(iedel) shears. They preferentially occur in the overlap zone between two parallel R shears and often connect these two R shears. They may develop with or after R shears.

P shears are synthetic minor faults symmetrically oriented to the R shears with respect to the fault plane. P shears also form an *en échelon* array contemporaneous

with R shears or later as links between R shears. P-shears are contractional and accommodate fault parallel shortening as shearing proceeds.

P' shears conjugate with P shears but these have relative minor importance and are difficult to separate, in terms of orientation.

Y shears are micro faults sub parallel to the main fault, apparently the last to form. Riedel micro faults may all connect with one another to form a network of fractures in a narrow fault zone whose bulk borders are parallel to the main fault.

T-fractures (tension fractures) would form at +45 to a right-handed fault (Davis et al 2000).

This study deals with field observations, structural mapping and petrographic analysis of cataclastic shears in the amphibolite facies Precambrian garnetiferous biotite schists around Sawantwadi. Sindhudurg District, Maharashtra. The unique characteristic of these cataclastic shears is that they appear to stand out of the surrounding schistose rocks in the field and are easily visible in aerial photographs. No previous work exists on the characterization of these structures. The biotite schist country rock is multiply deformed and the study area chosen reportedly contains a NW trending major terrain boundary steep shear zone passing through it (Rekha and Bhattacharya, 2014). However, the present study is focused only on the brittle to brittle-ductile planar structures identified as cataclastic shears within the rocks and aims at understanding the tectonic significance of these structures through detailed structural, petrographic and geothermobarometric analyses.

AIMS & OBJECTIVES

The objectives of the study encompass the identification and structural mapping of cataclastic meso-scale features within the designated area. Additionally, it aims to characterize the microstructures present in the cataclasites and report on the mineral chemistry of the phases within them. Through these analyses, the study endeavors to infer the origin and significance of the cataclastic deformation observed in the study area.

AREA OF STUDY

The area being examined is situated in the eastern part of the Sindhudurg District, Southern Maharashtra. It is shown in the black box in Fig-1.4. The area is located between 85.5 km and 115 km north of Goa University. It is bounded by Madhkol in the west, Ghotos in the north, Kesari in the south & Vasoli in the east. The primary towns near the study area are Kudal, Sawantwadi and Kankavali, which are connected to Panjim, Pune, and Kolhapur by National Highway (NH-17). The entire SE, E, and NE sides of the study area are hilly and part of the ghat region, making it challenging to access by road. The coordinates bounding the area are $N15^{\circ}51'-16^{\circ}04'$ & $E73^{\circ}49'-73^{\circ}50'$. The area is shown in toposheet no. 47H/16/SE and 48E/13. According to the toposheet the contours are very tight and are equally spaced indicating steep uneven slopes.

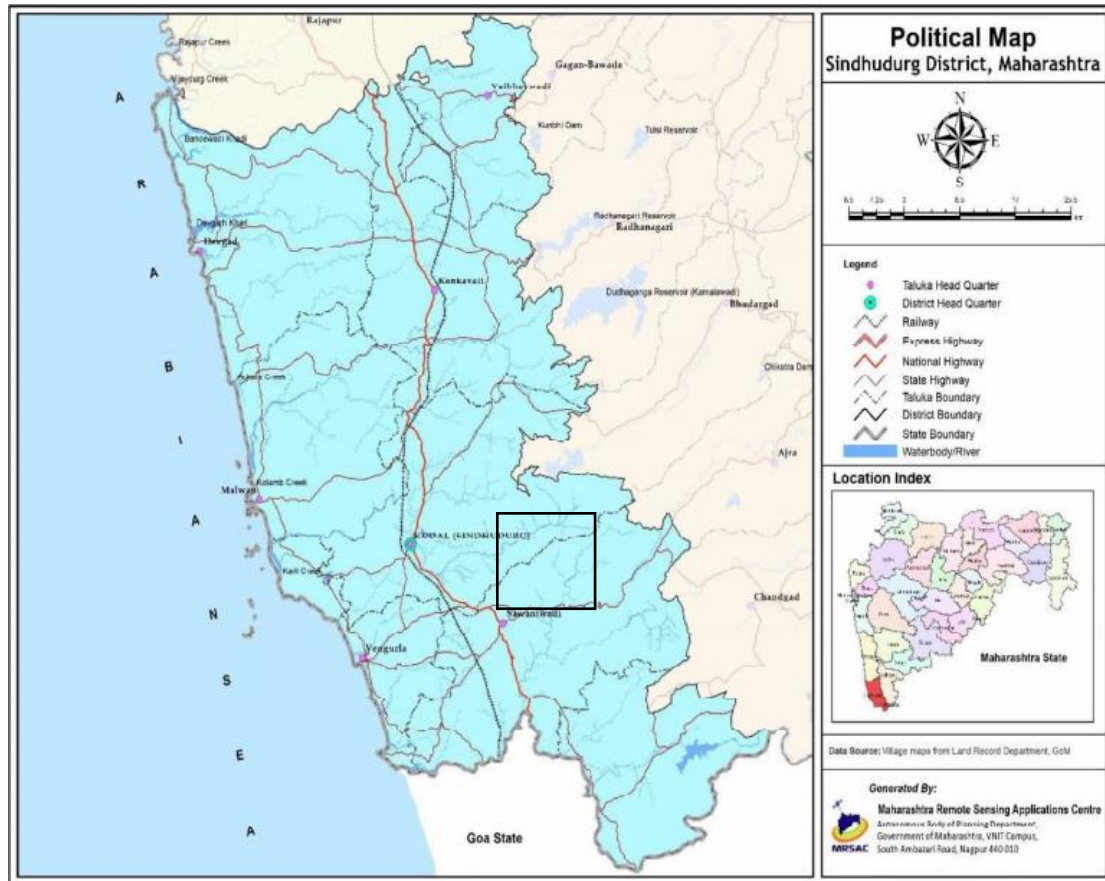


Figure-1.4 Political map of Sindhudurg district Maharashtra. The black box shows the area investigated in this study. (Source-Maharashtra Remote sensing application centre)

PHYSIOGRAPHY

The study area is a part of Sindhudurg district of Maharashtra is located in the Konkan region of SW India. The district is located between the N $15^{\circ}37'$ & $16^{\circ}40'$ and E $73^{\circ}19'$ & $74^{\circ}13'$. The district has a geographical area of 5207 sq km of which about 386.43 sq. km. is covered by forest, whereas the cultivable area is 3222 sq. km. The net sown area is 1522 sq. km. The district headquarters is located at Oros (Kudal). The district comprises two revenue sub-divisions viz: Sawantwadi and Kankavli. The eight talukas of the district are Sawantwadi, Vengurla, Kudal, Kankavli, Malvan, Deogad, Dodamarg, and Vaibhavwadi. The district is bounded in the north by

Sindhudurg district, west by Arabian Sea, east by Kolhapur district, and south by Goa State and Belgaum district of Karnataka State. The Western Ghats run through the district, forming a natural boundary between the district and the rest of Maharashtra. The district is primarily composed of hilly terrain, with an average elevation of 600-800 meters above sea level. The highest point in the district is the peak of Ramtirth, which is around 900 meters above sea level.

Drainage

All the major rivers originate from the Sahyadri ranges and drains from east to west into the Arabian sea. Almost every valley in the area has a perennial stream which serves as a rich source of water. The main rivers in the area are Londha Nadi, Bherambha Nadi, Marlonda Nadi, Vedganga river, Karli river & Terekhol river. The Drainage pattern is mainly dentritic to sub dentritic but some places sub parallel to parallel drainage pattern is also present.

The Karli river flows through the selected study area. Karli originates near Shivapur and flows in the south westerly direction and it is joined by major and minor streams of the area.

Climate

Climatic conditions in the district are strongly influenced by its geographical conditions. The district falls under the 'Assured and High Rainfall zone'. The climate is generally humid. The cold season is from December to February followed by summer from March to May. June to September is the southwest monsoon, while, October and November constitute the post-monsoon season. Being a coastal district, variation in the temperature during the day and throughout the season is not large. December is the coldest month with mean daily maximum temperature at 32.7°C and

the mean daily minimum temperature at 18.7°C. April is the hottest month. The relative humidity during the southwest monsoon is very high (86 to 90%). The relative humidity during winter and summer months is also above 57%.

METHODOLOGY

The area around NE of Sawantwadi was chosen for the study and route map was constructed using google earth. Preliminary fieldwork was carried out in January and March of 2024. A base structural map was available from Rekha & Bhattacharya (2014). As the selected area is rough and hilly terrain with dense forest cover, samples were collected wherever the outcrops were accessible and the coordinates were noted. During the fieldwork various structural elements such as foliation, orientation of cataclastic shears, cross-cutting relation of the shears, thickness and shear sense of these shears were noted.

The shears seen in the field occur as sets of sub-parallel inclined planes with different orientations and different sets intersect each other. These shear planes are more resistant to weathering and erosion, hence they stand out from the surrounding country rocks. The strike and dip data of each set of planes in the two locations was measured using a Clinometer compass and noted in the field notebook. Sketches of the features in the rocks were made on the field notebook and field photographs were taken using appropriate scale. Care was taken to orient the scale in the N-S direction. In situ rock samples were identified which contain the essential field structures for macro and micro analysis. A sledge hammer was used to break the rock. The broken pieces were packed in a plastic sample bags and the spot number was written on the bag. The samples collected and their particular purpose was mentioned in the field

diary. Stereographic projections and Rose diagrams were created by using GEORient software (version 9.5.0)

The rock samples collected were taken to the Hard rock lab and using rock cutting machine samples of size 2Cm ×6Cm were cut perpendicular to the foliation for petrographic study. These thin sections were observed under Nikon Elipse E200 microscope and photos were clicked using digital camera D5100. EPMA data of silicate minerals from each rock type was obtained from the EPMA Facility at the Department of Earth Sciences, IIT Bombay. The structural formulae were calculated for each mineral. The different data sets were collated to understand the tectonic importance of the cataclastic shears in the area.

CHAPTER II : Background Geology

Geological Features of Sindhudurg

Situated within the Konkan region, between the Arabian Sea and the Western Ghats, Sindhudurg district boasts a diverse geological landscape. Initially classified as the "Older Metamorphic Series" by Wilkinson in 1871, these rocks were later grouped by Foote in 1876 into the "Gneissic Series" and Dharwar System. Iyer (1939) further categorized the pre-trappean rocks of South Konkan and Maharashtra under the Metamorphic and Unmetamorphosed "Kaladgi Series". Kelkar (1956) identified two main groups of Archean metamorphic rocks, distinguished by a thrust contact between them. Group I includes granite gneiss, quartzites, mica schists (garnet), staurolite and kyanite, biotite, and hornblende granulites, while Group II consists of coastal rocks like crushed conglomerate, phyllites, and ferruginous quartzites. Ghodke (1983) classified the metamorphic rocks of Sindhudurg as part of the Banda Group, suggesting their equivalence to the middle and upper divisions of the Dharwar Supergroup. Additionally, Naqvi & Rogers (1987) noted the presence of schists along the Western coast of India and Goa, possibly extending northward into Karwar. However, studies primarily focused on the northwest, west, and far south of the district, with few attempts made to establish the interrelationship between the supracrustal rocks of these areas. The lithology of the region is characterized by a sequence of metagreywackes and amphibolites intruded by various generations of granitoids, interspersed with banded iron formations (BIF) and quartzites. The southern part of the district forms the northwestern section of the highly deformed and evolved Dharwar Craton, where supracrustal rocks exhibit superimposed deformation (Deshpande & Pitale 2014; Rekha & Bhattacharya 2014).

Rekha and Bhattacharya (2014) recently identified two distinct shear zones within the study area: a NNW-trending Northern Shear Zone (NSZ) characterized by gently dipping foliation and open folds with NW-trending axial planes, and a WNW-trending Southern Shear Zone (SSZ) featuring subvertical to steeply south dipping foliations and reclined folds with WNW-trending axial planes. The rocks in the study area have been dated as Precambrian crystalline rocks through Pb-monazite geochronology. South of the SSZ, ages of the Goa Schist Belt range between 2.4 and 2.6 billion years (Ga), with a statistical peak of 2520 ± 18 million years (Ma) and a subsidiary Paleoproterozoic age population of 2366 ± 21 Ma. Additionally, the metamorphic age of greenschist facies Supracrustals in the Goa Schist Belt of the Western Dharwar Craton (WDC) has been estimated to be approximately 2.5 Ga. In the schists between the SSZ and the NSZ, the dominant statistically resolved ages in monazites are Paleoproterozoic (2385 ± 14 Ma, 2192 ± 17 Ma, and 1872 ± 14 Ma), with a minor population of Mesoproterozoic ages (~ 1460 Ma). Notably, the 2.5-2.6 Ga age in the greenschist facies Supracrustals of the Goa Schist Belt south of the SSZ is uncommon in samples north of the SSZ. The lithologies north of the NSZ exhibit Paleoproterozoic ages (2303 ± 12 Ma, 2198 ± 15 Ma, 2088 ± 16 Ma, 1953 ± 22 Ma, and 1788 ± 27 Ma), consistent with those observed between the SSZ and NSZ. The prominent Mesoproterozoic mean age (1673 ± 15 Ma) in this region is attributed to spot ages obtained from quartzite.

Fluvio-Marine deposits Laterite		Tertiary to Recent
Deccan Traps	Basalt (lavaflores and intrusives)	Cretaceous to Eocene
Unconformity		
Intrusives	Dolerite /basalt dykes Synite/Pegmatite /quartz veins Gabbro/Dolerite Pluton Pat granite (?) Meta Gabbro / Meta dolerite	Equivalent to Chitradurga Group of WDC
Intrusive contact		
	BHQ Metapelites	
Spracustrals	Metabasalts/Actinolite/Hornblend Schist Quartzites	Archean to meso proterozoic
Tectonic contact		
Basement Gneissic Complex		Peninsular Gneissic Complex

Table 2.1:-Lithostratigraphy of the sindhudurg district.

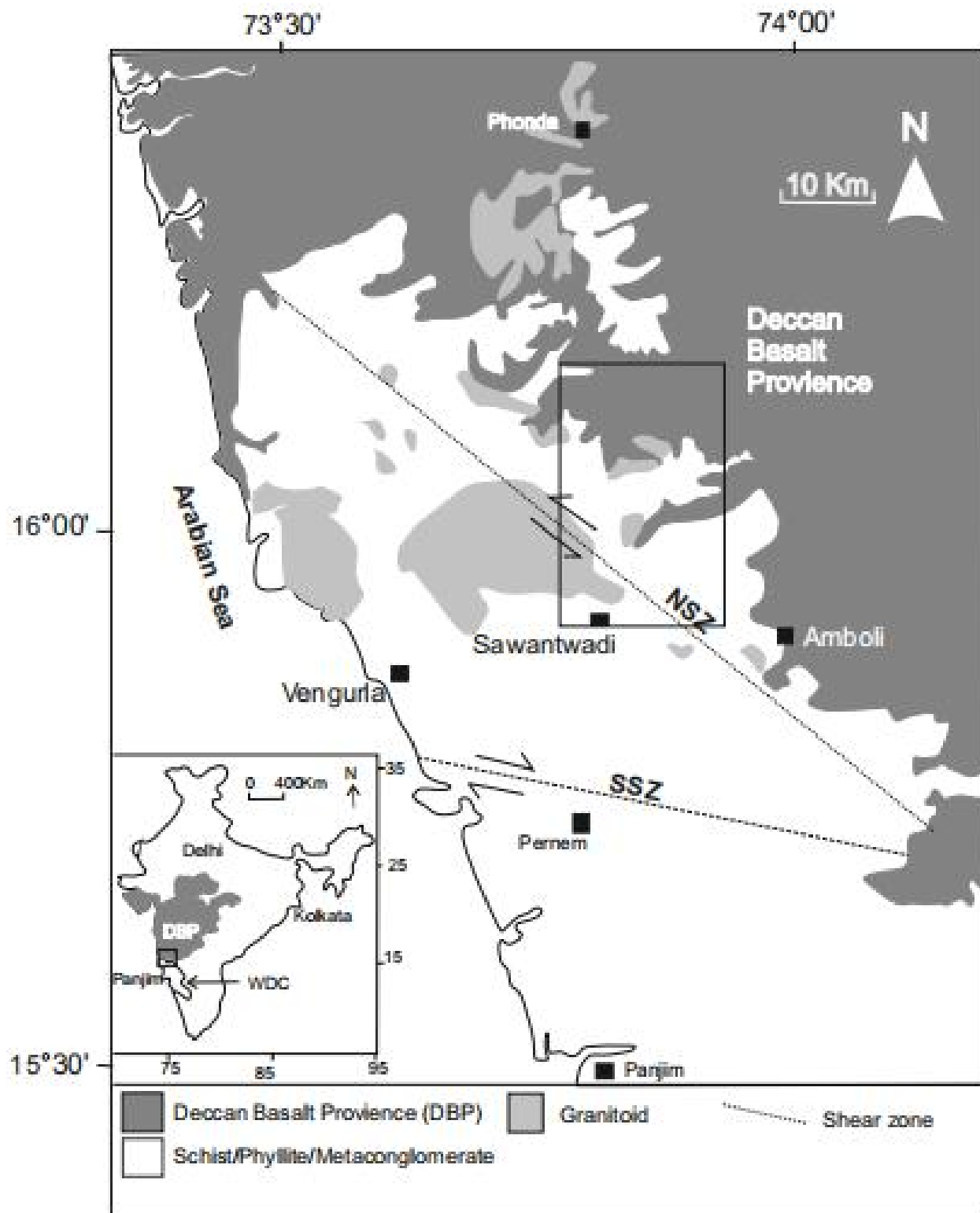


Figure.2.1: Generalized geological map of Pernem (Goa)-Phonda (Maharashtra) corridor adopted from Rekha and Bhattacharya (2014) .with the study area marked on it.

Geology Of The Study Area

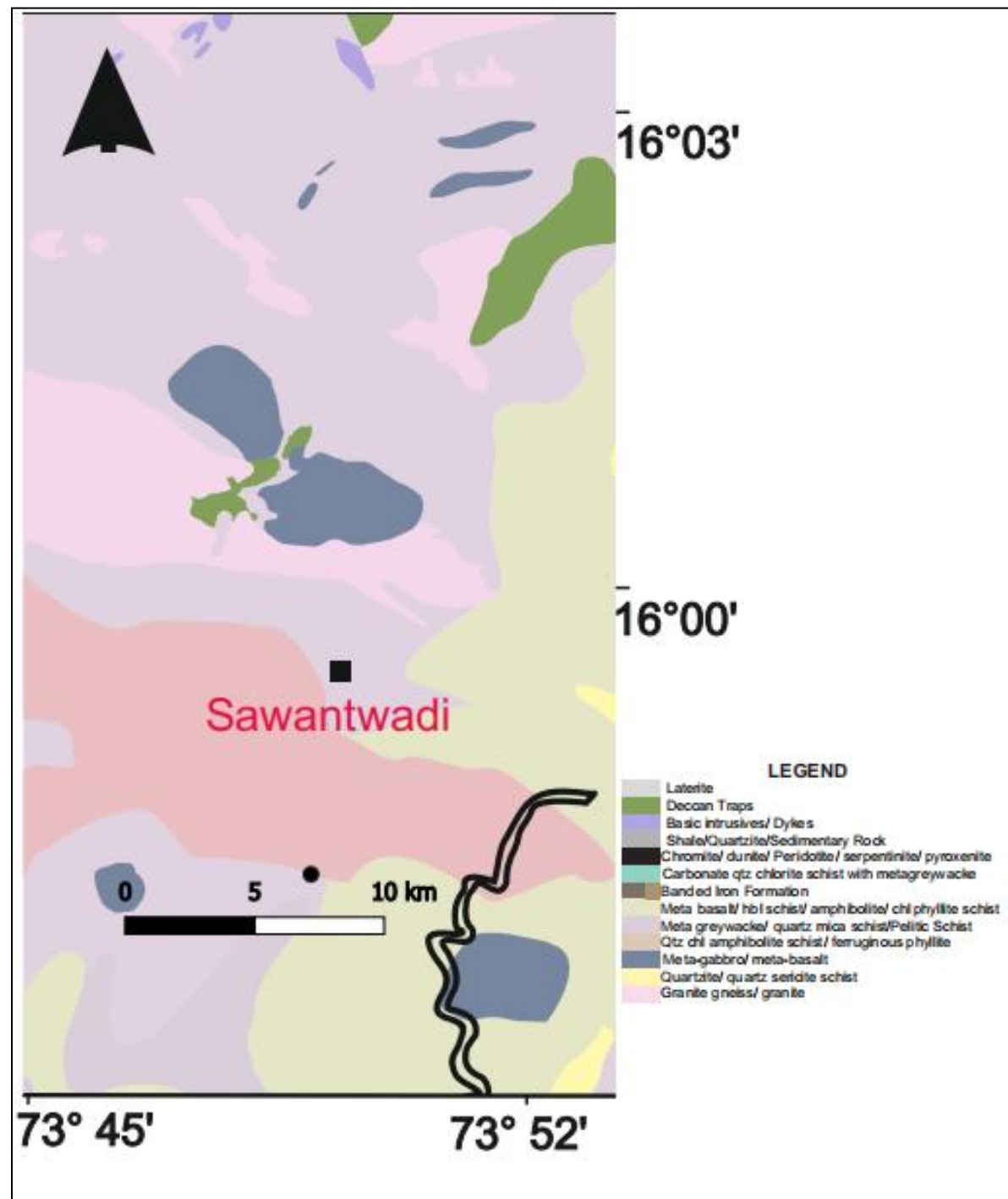


Figure.2.2: Generalized geological map of Pernem (Goa)-Phonda (Maharashtra) corridor adopted from Rekha and Bhattacharya (2014)

The study area is located East and north east of Sawantwadi and It is bounded by Madhkol in the west, Ghotos in the north ,Kesari in the south & Vasoli in the east The ENE side of the study area is a part of the Amboli Ghat. The rocks in the study area are metamorphic rocks which predominantly comprise of biotite schists and biotite gneisses. These lithologies are considered as a part of the Archean supracrustal basement of the WDC. The biotite schists and gneisses are garnetiferous in several locations in the area and have undergone many deformation as manifested by presence of crosscutting foliations and folds.

The Deccan traps extend into the area which are identified by their basaltic composition and upper cretaceous to lower Eocene age. The biotite schists are intruded by basic intrusives of dolerite which have been metamorphosed to meta gabbro/ meta dolerite.

The rocks have experienced at least four deformation episodes and associated folding events. There is a steeply to moderately dipping N-S foliation which is folded and forming steeply dipping E-W foliation. The E-W fabrics are later folded with to N60 fabrics. The youngest fabric is the N120 which formed when the N60 fabric is seen curving into the N120 orientation. In this area study been made to establish the detailed metamorphic and deformation history as well as to correlation of the area, although the available information is limited .

CHAPTER III :FIELD CHARACTERISTICS & STRUCTURES

The rocks encountered in the study area consist of mainly dark colored, fine to medium-grained biotite schists and granites. In several locations within the area, the biotite schists were interbanded 10s of cm thick layers of darkgreen bands comprising hornblende, plagioclase and garnet which could be identified with naked eye. In the schists, garnets occur as pink to reddish brown euhedral porphyroblasts, which show a variation in size from 1 mm to 2 cm.

The rocks of the study area show complex deformational history and the study of interrelationship in terms of structural elements in the biotite schists have revealed that the area exhibits at least four deformation fabrics as.

- Steeply dipping N-S Foliation
- Steeply dipping E-W Foliation
- Steeply dipping N60 Foliation
- Moderately dipping N120 Foliation

These foliations are marked on the lithological map of the study area for the 13 locations selected (Fig. 3.1). Foliations are seen as the parallel alignment of micaceous minerals in the rock and imparts to it a lepidoblastic appearance. Due to the hilly terrain, lack of good exposures and scarcity of roads, the majority of the data could only be acquired from western part of the study area where the outcrops were easily accessible along the road side.

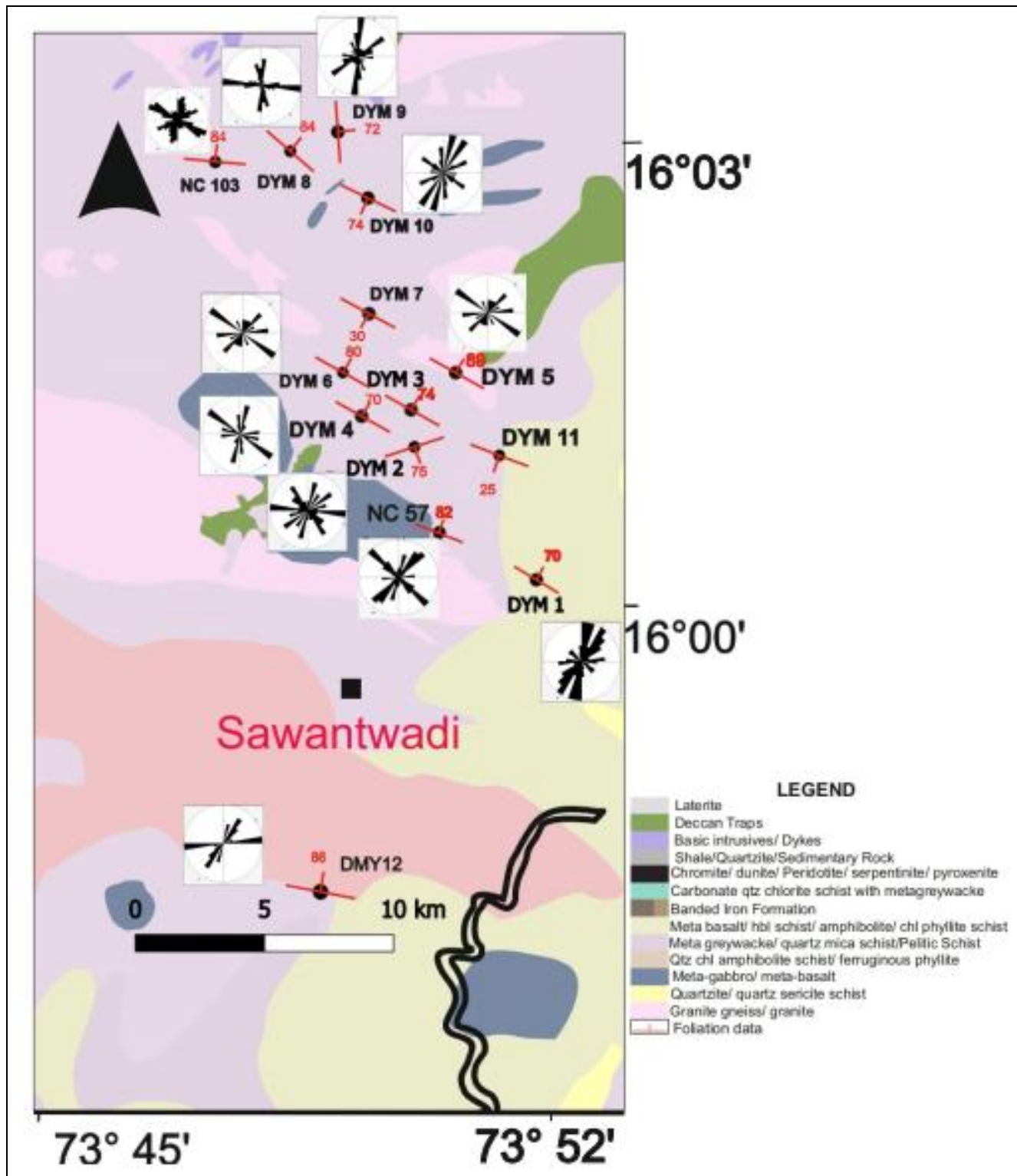


Figure.3.1: Lithological map of the study area showing the locations selected for detailed investigations. The penetrative foliation for each location is shown in red. The orientation of cataclastic shears in each location is depicted in a rose diagram beside the location. modified after Rekha & Battachrya 2014

Planar features, mm to cm thick, occur in various crisscrossing, intersecting sets within all the biotite schists and granites in the study area (Fig. 3.2). These planar features were labeled as “shear fabrics” (Rekha et al., 2014) or “boxwork structures” (V. Venugopal 2023, F. Azhar 2022) in previous studies. They generally stand up as ribs out of the country rocks because of relatively higher resistance to erosion so they are very distinctive and can be traced easily. These planar features are visually comparable to deformation bands reported in low grade sedimentary rocks (cf. Navajo sandstone (Davis et.al 2000), but in the present area, they occur in metamorphic rocks. The planar features vary in composition. In some sets, they appear to have the same mineralogy of the host rock, while others show presence of greenish, blackish as well as lighter colored minerals than the surrounding parent rock. Close inspection with lens and after petrographic investigations (See Chapter 4), it was concluded that these planar structures are cataclastic shear bands as they are associated with brecciation, and contain angular broken fragments of the host rock.

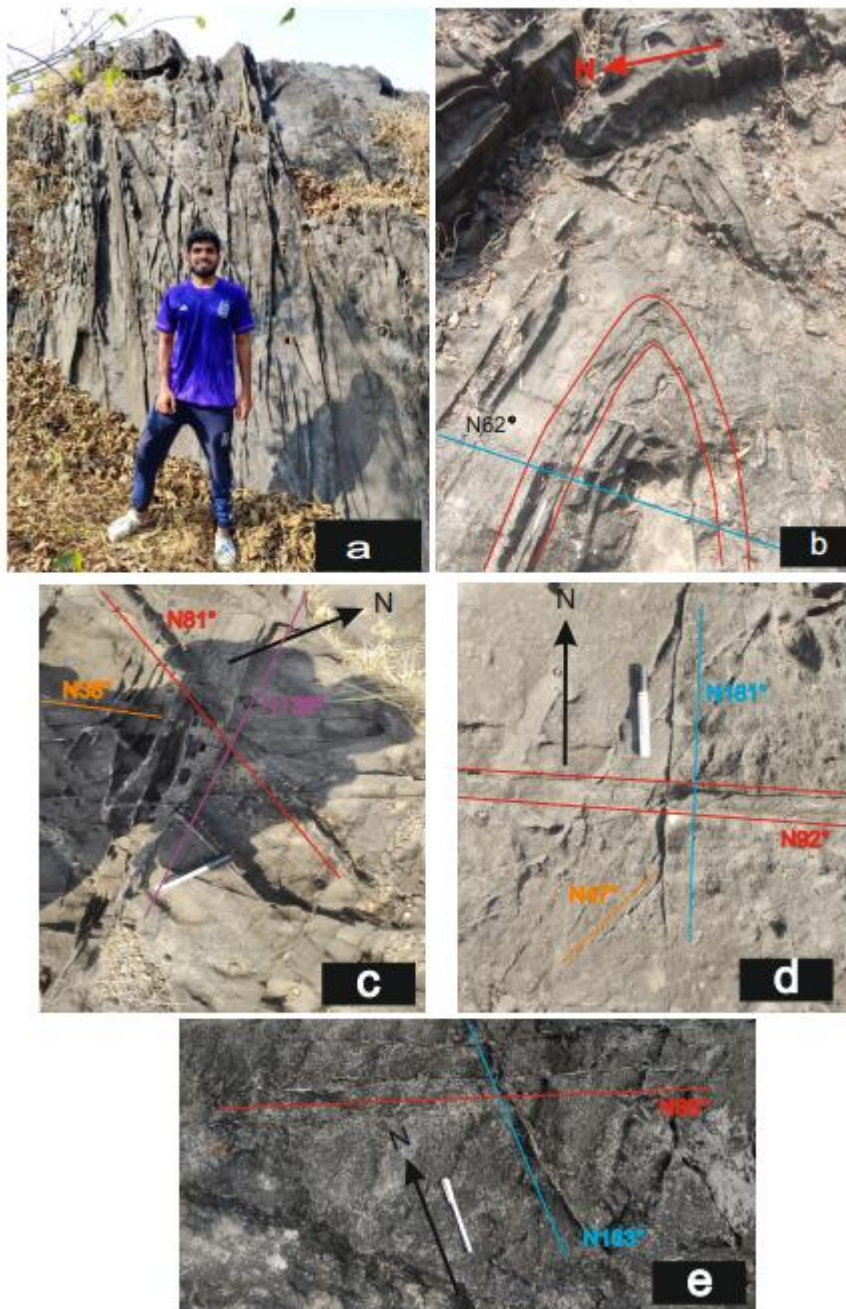


Figure 3.2- Photographs showing cataclastic shears in biotite schists interlayered with cm thick calc-silicate layers in the field. (a) inclined cross-sectional view (b) plan view of a folded calc-silicate layer being cross by N62° oriented shear. (C) & (d) plan view photographs of the E-W oriented calc-silicate band being intersected by various shears.

The cataclastic shears are generally continuous across entire outcrops. Refraction of orientation or termination of the cataclastic shears is observed when there are changes in mineralogy, especially in the schists (Fig. 3.3). The shears are better developed in the stronger lithologies and lithologies containing abundant garnet.

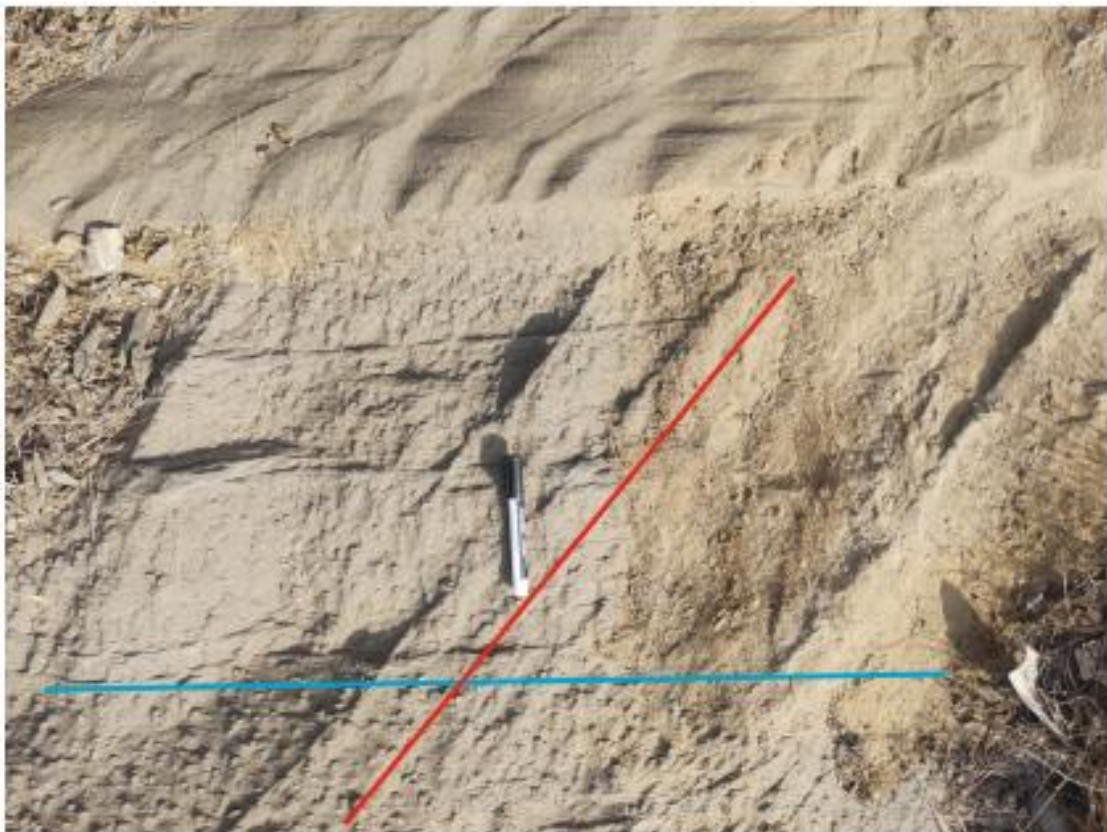


Fig 3.3- Plan view photograph of termination of cataclastic shear oriented in $N60^\circ$ within a garnet bearing biotite schist, at the contact of garnet absent schist. Pen measure 14 cms, points North.

Cataclastic shears with different orientations are present in most exposures and usually are sub-vertical and appear to crosscut each other (Fig.3.2). Detailed measurement of the orientations of the cataclastic shears were carried out in 11

locations of the area (Fig. 3.1). These cataclastic shears can be mistaken with the interlayered calc-silicate banding within the schists, which also stand out from the host rock. However, these layers are usually 10s of cms thick and are parallel to the penetrative ductile foliation in the rock. There are two outcrops where no cataclastic shears were observed (DYM 7 & DMY 11). The rocks at these locations were more micaceous in mineralogy compared to the other locations, possibly hinting to a rheological control on the formation of the cataclastic shears in the study area.

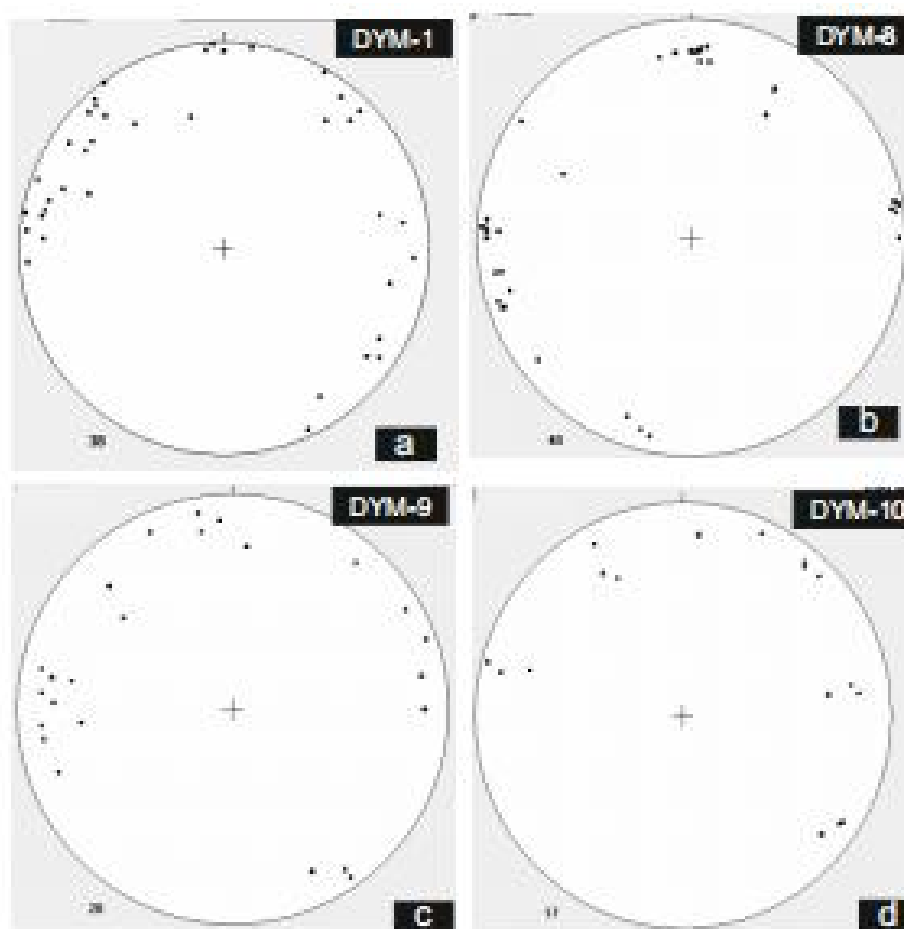


Figure 3.4-Stereonet plots for Outcrops in the north eastern part of the study area.

DYM-01 the outcrop shows a steep foliation which is oriented N120° with majority of the cataclastic shear planes are striking North -South with NE as the second major set , some shear are developed a along the foliation but these are not very

prominent .DYM-08 also similar characteristics of foliation as that of DYM-01 but the set of shear dominating thus out crop is North South and East West oriented.DMY-09 show orientations of cataclastic shear planes along the foliation of the rock with a subsidiary set oriented in NE direction.DYM-10 has all the major orientation of shears all these shears are very steep.Majority of these poles are present in northern part of the plot indicating these planes are steeply dipping south.

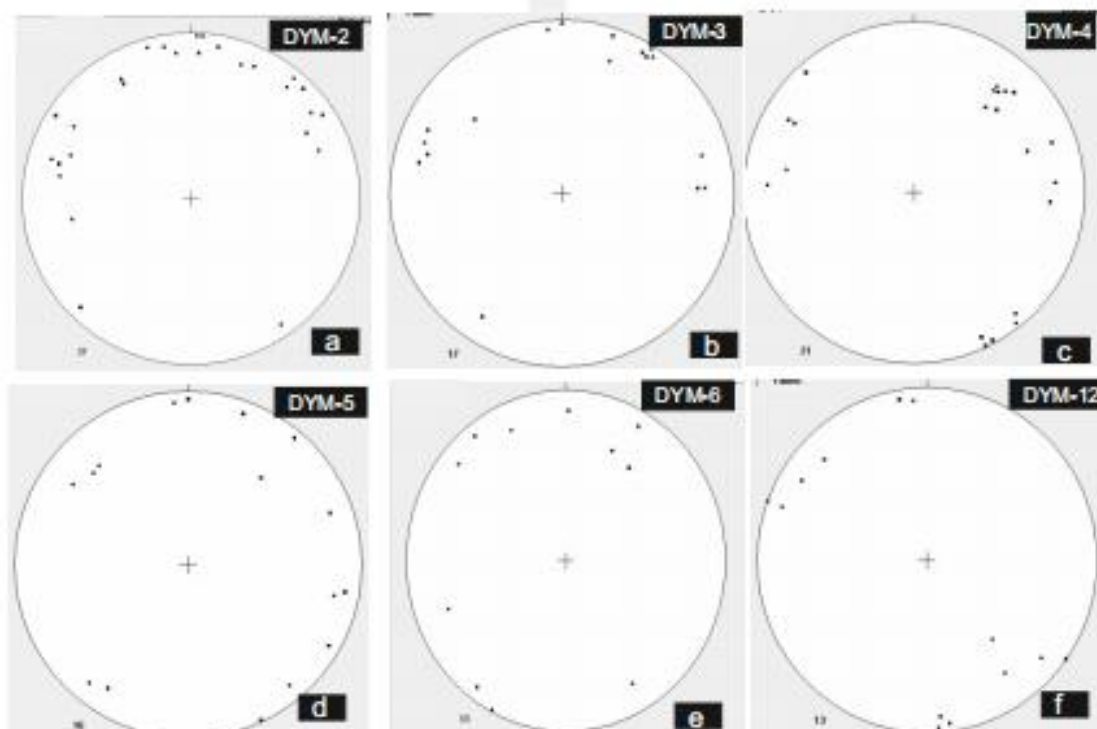


Figure 3.5 : Stereonet plots for Outcrops in the central part of the study area showing SW foliation.

DYM -2 plots show a steep striking planes which are oriented in East west direction also a set of shear planes are oriented along the steep foliation fig 3.5(a)DYM 03 & DYM 04 are similar outcrops located very close to each other with almost similar foliation is present in both location but there are N-S strikeing shears in DMY-03 but this shears are absent in DMY-04 and both this locations have 1 set of shears strkeing along the foliation of the rock.fig 3.5(b & c).the stereo plots for DYM 06 & DYM 05

are almost similar, there is 1 set of dominant shears along the defoliation of the rock while 1 set of conjugate shear is formed by east-west & NE oriented shears figure 3.5 (d & e). DYM 12 is the only outcrop located in the southern part of the study area. The two major orientations of planes are in East-West and NE. These planes are very steep. fig 3.5 (f)

Towards the north of study area the N-S and E-W orientation of the cataclastic shears is dominant while the N120 shear is dominant in the central part of the study area with a sub shear oriented at N60°. A dominant cataclastic shear set is parallel to the penetrative foliation in every outcrop investigated, indicating that the cataclastic shear formation may also be associated to pre-existing planes of weaknesses, such as foliations in the rocks.

The displacement across cataclastic shears is usually in the order of a few millimeters, rarely up to a few centimeters (Fig. 3.6, 3.7). For this reason it is not always possible to detect offsets of layering across every band, especially when the bands are not completely exposed or there is compositional layering of the parent rock. However, close inspection of the offsets wherever possible indicates that there is no consistency of the offsets across the cataclastic shears of any specific orientations (Fig. 3.7). Dextral and sinistral offsets were seen across the same shear set in the same outcrop as well (Fig. 3.7)

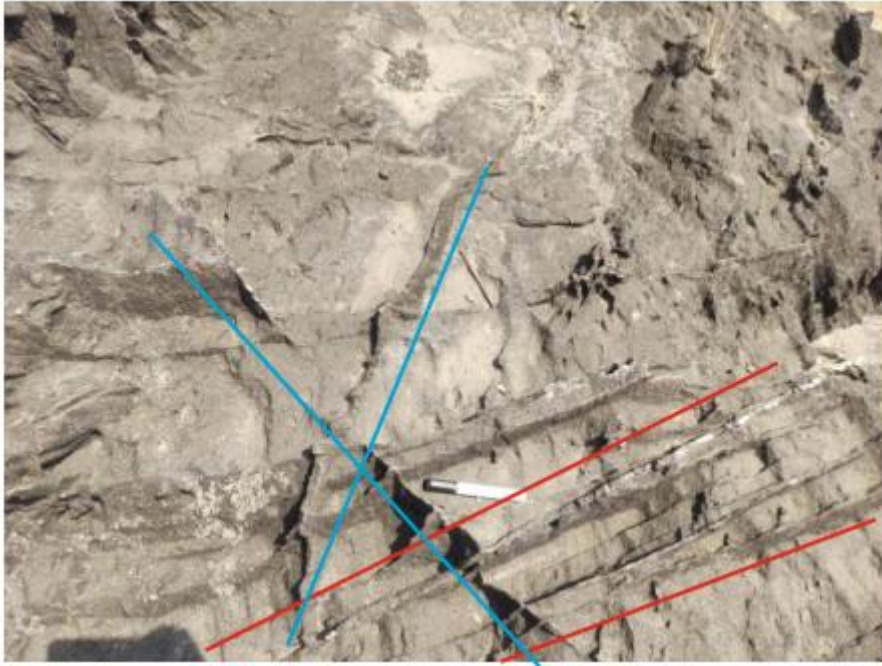


Figure 3.6 Plan view photograph of the cataclastic shears oriented N140° (parallel set marked in red) & conjugate shears (marked in blue) of N60° & N110°. Note the dextral shear sense associated with the N140 shear displacing the N60 shear, and the abrupt termination of the N140 shear against the N60 shear.

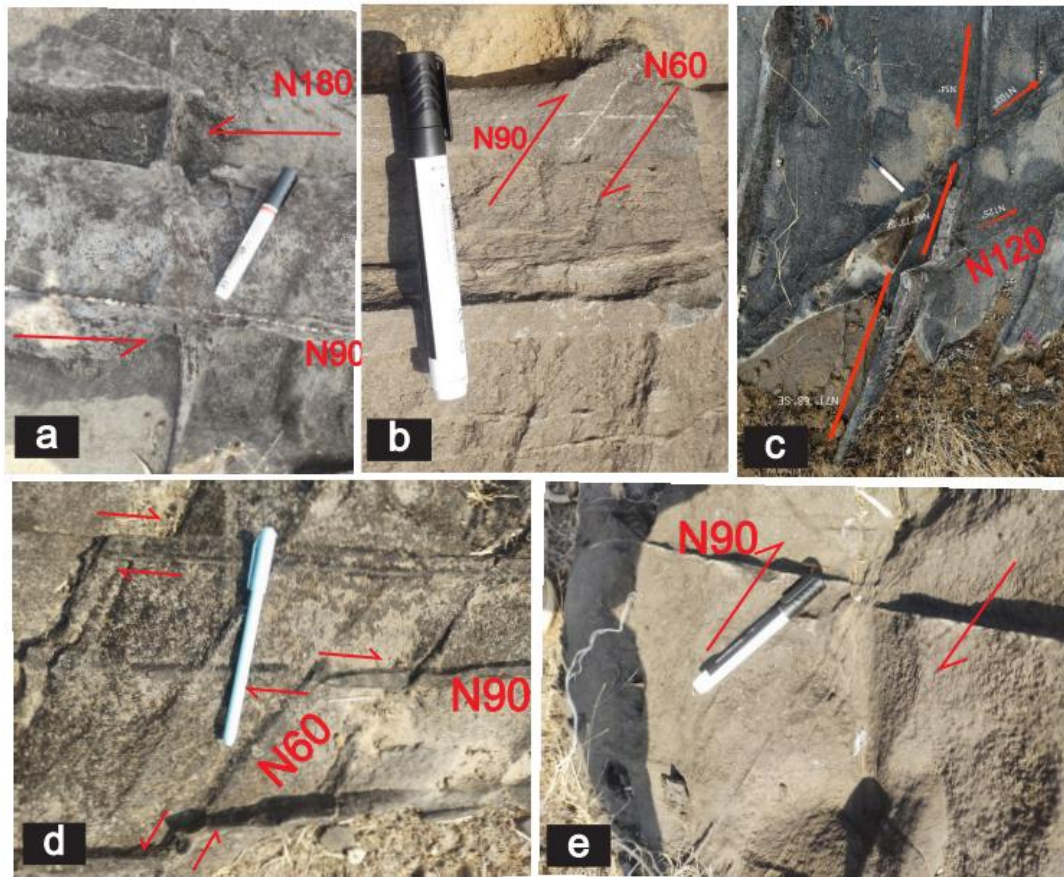


Figure 3.7-Shear senses associated with different cataclastic shears.(a)Plan view photograph of North -south shears showing a dextral fabric.(b)Plan view photograph of N60° shear showing a dextral sense with N90°.(c)Plan view photograph of N60° shear showing a sinistral shear sense.(d)Plan view photograph of Intersection of N60° & N90° shear showing both sinistral and dextral shear sense (e)Plan view photograph of N90° shear showing dextral shear sense.

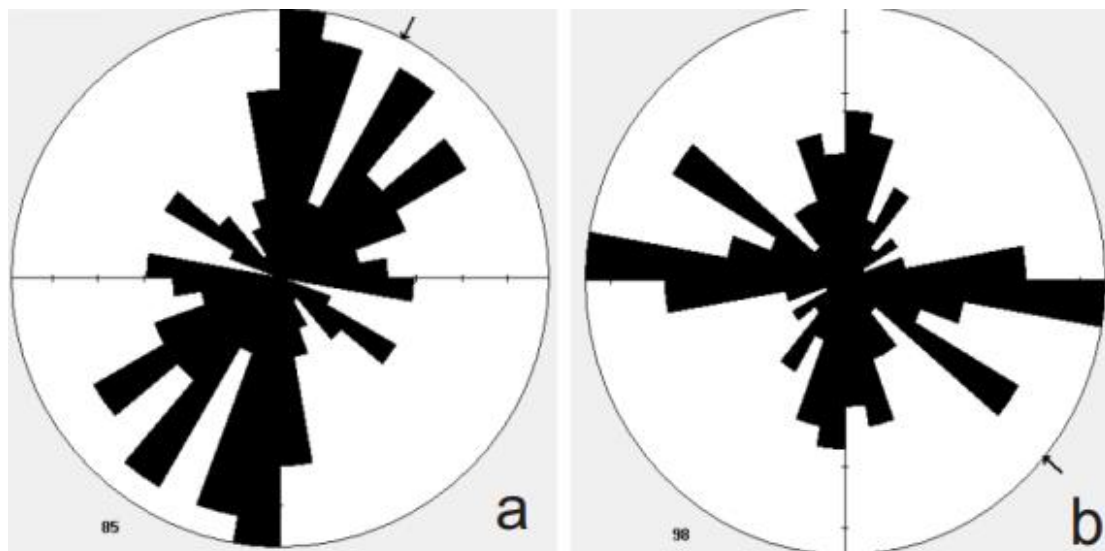


Figure 3.8 -(a) Rose diagram for outcrops showing major orientation of cataclastic shears as North-South.(b) Rose diagram for outcrops showing major orientation of cataclastic shears as South east.

The rose diagram for the major N- S oriented cataclastic shears shows a conjugate set of shears but the major conjugate set is located in the North Eastern corner marked by N-S & NE shears. There is another subsidiary set which is not developed completely but shows an SE orientation. Fig 3.8 (a). The outcrops showing prominent cataclastic shears oriented N120° shear were taken to create a rose diagram showing an east-west shear & N 120° shear form a set of conjugate shears. Here N-S can be the subsidiary shear.

CHAPTER IV: MINERAL CHEMISTRY & MICROSTRUCTURES

General petrology of the region.

The study area located in the Sindhudurg district of Maharashtra is composed of newly discovered suite of Paleoproterozoic/Mesoproterozoic amphibolite facies supracrustal rocks and foliated granitoids. The biotite \pm chlorite schists and hornblende/biotite amphibolites, commonly garnet-bearing, are the dominant lithologies in the corridor. The frequency and size (subcentimeters in diameters) of garnet porphyroblasts in the schists/amphibolites increases southward to the cratonic fringe. schists/amphibolites that exhibit several generations of folds and tectonic fabrics, the granitoids possess a single tectonic fabric. The schistose rocks have an intercalated calcic layer which is aligned with the foliation of the various outcrops. The first is a North - South steep fabric which was later folded to an East -west fabric there after this fabric was folded to folds with axial plane trending N60°.

The schistose rocks have many secondary features like quartz veins, sheath folds, cataclastic shears. The granites are Grey to pink in colour showing some fabric. mineralogy of the granites include Quartz, Feldspar, Hornblende, Epidote and biotite. The following sections describe the petrographic features of each rock type especially the microstructures associated with the cataclastic shears that traverse through the rocks. EPMA data was obtained from the EPMA Facility at the Department of Earth Sciences, IIT Bombay for silicate minerals from each rock type. The structural formulae were calculated for each mineral and the petrographic description includes the observations and inferences from this data.

Petrography of Cataclastic shears

For the Petrographic study of the cataclastic shears, the samples were cut perpendicular to the shear. The slab shows two distinct bands of lithologies. One is characterized by light colour minerals while the other is a dark layer. If we have a closer look, these two bands have a greenish mineralogy which is separating them. The orientation of the shears is clearly visible in the hand specimen. For a closer identification of the mineralogy, textures, orientation of the shears & Identifying change in secondary mineralogy of the shears in the two different layers. (Fig 4.1)

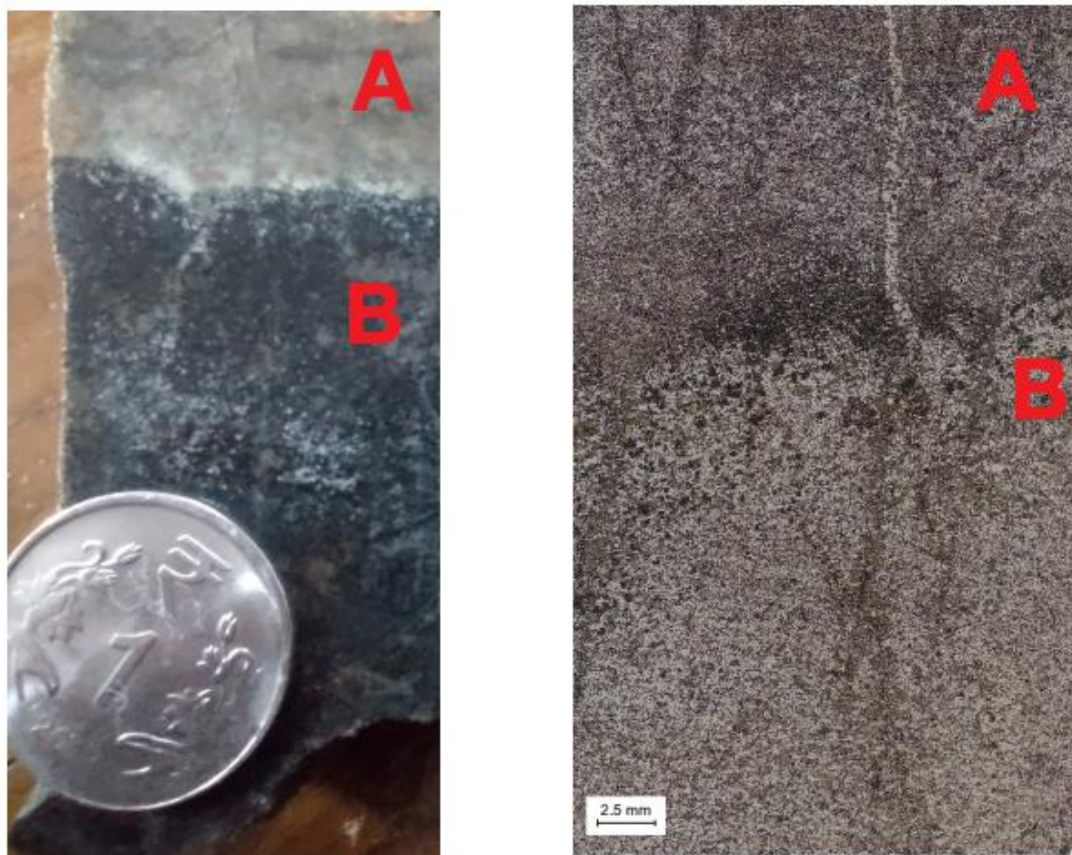


Figure 4.1-Photograph of hand specimen & thinsection showing two different lithologies marked as (a) light / Calcic mineralogy (b) biotite schists with garnets. [In the thinsection the b layer is further divided based on mineral composition b1- Garnet+biotite +hornblende, b2-plagioclase+hornblende+clino pyroxene & b3- plagioclase +clino pyroxene

Layer a

The white layer is composed of calcite, Garnets, Scapolite, Pyroxene, Epidote, A cloudy matrix, Sphene and Quartz is present as veins.

The garnets are non-coronal, highly fractured, isolated grains, but few grains have aligned in the same orientation and are close to each other and portray varying metamorphic textural features from xenoblastic to sub-idioblastic to idioblastic indicative of changing pressure and temperature conditions during its growth. The Grains are highly fractured. The Garnets are accompanied by the inclusion of quartz, pyroxene and Scapolite. Pyroxene reaction rims are observed around garnets. Along the shear the garnets are showing chlorinisation & precipitation of mica.

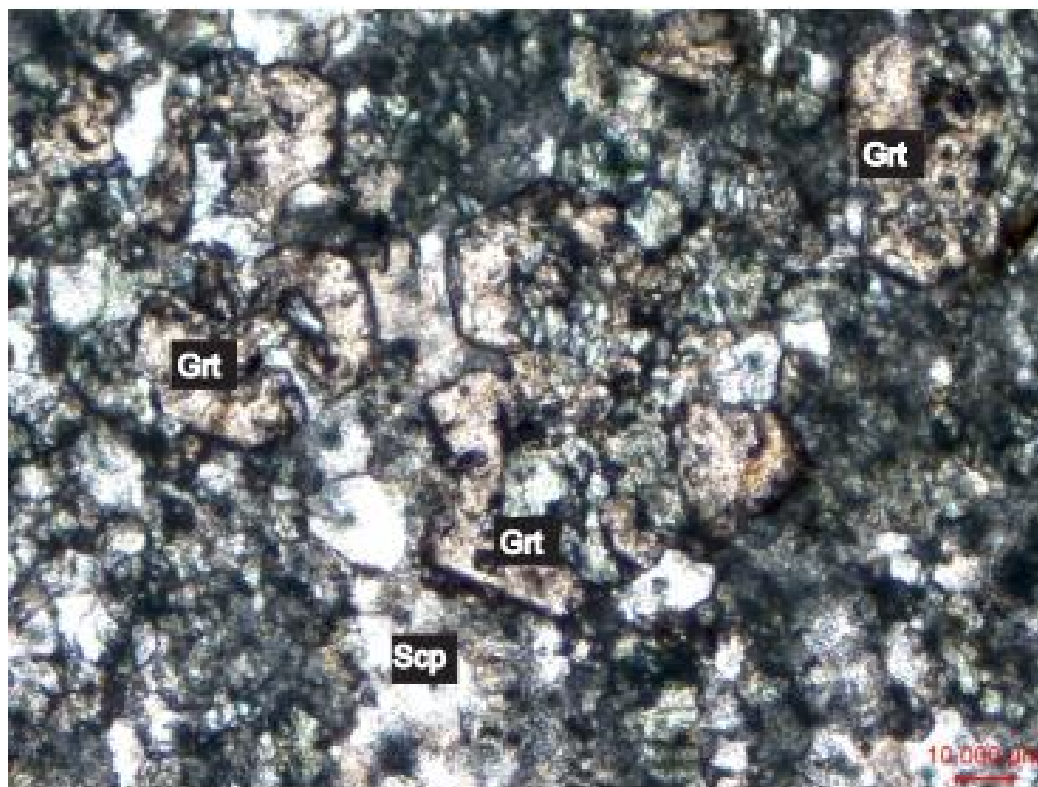


Figure 4.2 -Plane polarized photomicrograph showing Garnet surrounded by Diopside and scapolite, garnets are characterizing an orientation

Garnets grains in the a layer (34 ,36& 37) are rich in Ca 21-22% and FR. Compared to the garnets in the matrix layer. Garnets in the calcareous layer are highly fractured and have inclusions ,moreover the garnets have aligned themselves in this layer ,when the shears passes through this grains.Garnets show subrounded grain boundaries showing alignment within the matrix.

Table No 4.1: Mineral chemistry and Structural Formulae of Garnet based on 12 oxygen

oxides	Grt									
	21	22	23	34	35	36	37	62	63	64
SiO2	37.97	37.94	38.01	38.51	38.01	38.14	38.51	37.59	37.91	38.05
Al2O3	20.64	20.31	20.69	20.66	20.52	20.49	20.53	20.78	21.06	20.94
TiO2	0.01	0.11	0.02	0	0.1	0.11	0.03	0	0	0
FeO	21.31	21.06	21.9	17.57	20.71	16.82	17.59	30.29	30.03	31.33
MnO	4.25	4.25	4.95	1.66	1.66	1.48	1.54	2.09	2.14	2.1
MgO	1.06	1.02	1.11	0.59	0.82	0.55	0.6	2.45	2.73	3.07
CaO	14.68	14.79	13.25	21.07	17.55	21.47	20.68	6.13	6.64	5.12
Na2O	0.06	0.01	0.04	0.06	0.04	0.07	0.02	0.04	0.08	0.02
K2O	0.03	0.05	0.01	0.03	0.04	0.02	0	0.02	0	0.02
Cr2O3	0.03	0	0.02	0.01	0	0	0	0.04	0.01	0.06
P2O5	0.06	0	0.05	0.03	0	0.03	0.02	0	0	0.05
BaO	0	0	0	0	0	0	0	0	0.04	0
Calculated for 12 oxygen										
Si	3.01	3.02	3.02	3.02	3.02	3.01	3.03	3.02	3.01	3.02
Al	1.93	1.91	1.94	1.91	1.92	1.91	1.9	1.97	1.97	1.96
Ti	0	0.01	0	0	0.01	0.01	0	0	0	0
Fe	1.41	1.4	1.45	1.15	1.37	1.11	1.16	2.04	1.99	2.08
Mn	0.29	0.29	0.33	0.11	0.11	0.1	0.1	0.14	0.14	0.14
Mg	0.13	0.12	0.13	0.07	0.1	0.06	0.07	0.29	0.32	0.36
Ca	1.25	1.26	1.13	1.77	1.49	1.82	1.74	0.53	0.56	0.43
Na	0.01	0	0.01	0.01	0.01	0.01	0	0.01	0.01	0
K	0	0.01	0	0	0	0	0	0	0	0
Cr	0	0	0	0	0	0	0	0	0	0
P	0	0	0	0	0	0	0	0	0	0
Ba	0	0	0	0	0	0	0	0	0	0
XFe	0.46	0.46	0.48	0.37	0.45	0.36	0.38	0.68	0.66	0.69
XMn	0.09	0.09	0.11	0.04	0.04	0.03	0.03	0.05	0.05	0.05
XMg	0.04	0.04	0.04	0.02	0.03	0.02	0.02	0.1	0.11	0.12
XCa	0.41	0.41	0.37	0.57	0.49	0.59	0.57	0.18	0.19	0.14

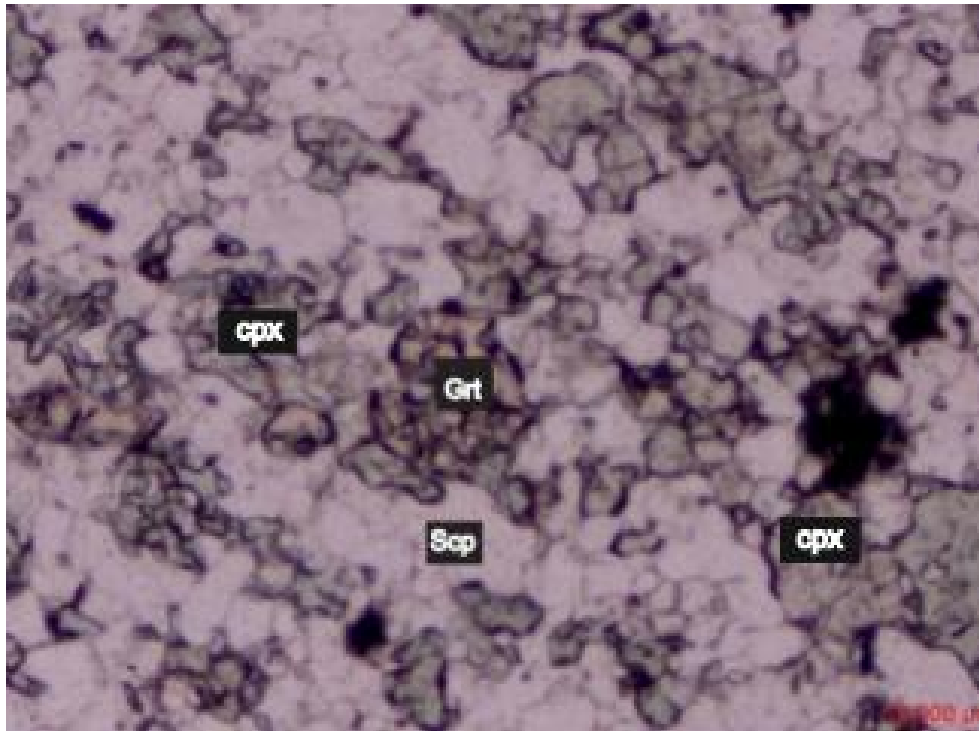


Figure 4.3-Plane polarized photomicrograph showing Garnet surrounded by Diopside

Calcite grains have a low to high relief and shows twinkling effect. The crystals are anhedral and have a rhombohedral cleavage. It is anisotropic and has higher order colors and exhibits symmetrical extinction. The ground mass within in this layer shows similar twinning compared to that of calcite .The Calcite grains are recrystallizing around the previously formed crystals of Garnet and Epidote.

Pyroxene is pale green in colour and has 1 set cleavage with subhedral grain shapes with sinusoidal grain boundaries. Shows higher order birefringence colors with inclined extinction under crossed polarized light.Compositional it is rich in Ca 22% & from the plot we can call it Diopside.Grains of pyroxene are present as inclusions in this band and also this grains are linearly arranged.The shear has also penetrated through these grains.Pyroxene from rim around Garnets.

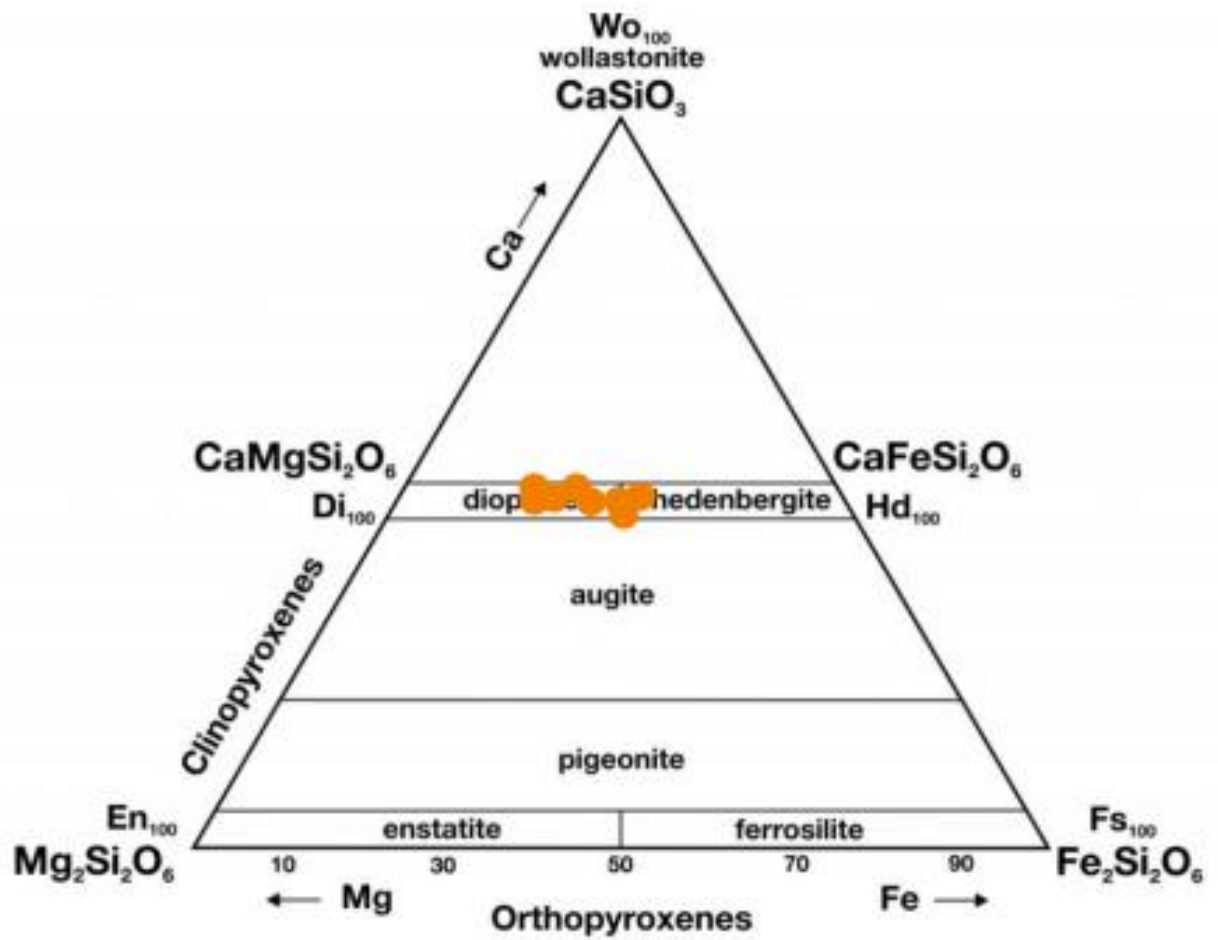


Figure no 4.4-Ternary plot for Classification of pyroxenes.

Table No 4.2: Mineral chemistry and Structural Formulae of Pyroxene based on 12 oxygen

SiO ₂	53.96	52.23	51.86	52.26	51.93	52.53	51.48	52.42
Al ₂ O ₃	0.63	0.73	0.92	0.97	0.85	1.11	0.76	0.72
TiO ₂	0.02	0.08	0	0.08	0.24	0	0	0.05
FeO	13.33	12.57	12.71	12.52	13.18	11.74	14.25	12.92
MnO	0.62	0.6	0.4	0.45	0.57	0.37	0.17	0.67
MgO	8.96	9.67	9.67	9.92	9.35	10.21	8.72	9.61
CaO	22.79	23.4	23.76	23.15	23.16	22.99	23.42	23.24
Na ₂ O	0.33	0.34	0.37	0.45	0.32	0.36	0.32	0.4
K ₂ O	0.05	0.01	0.05	0.04	0	0.25	0.09	0
Cr ₂ O ₃	0.01	0.07	0	0.06	0.04	0.05	0.08	0.01
P ₂ O ₅	0	0	0.01	0	0	0.02	0	0
BaO	0	0	0	0	0	0	0.01	0
Ions								
Si	2	2	2	2	2	2	2	2
Al	0	0	0	0	0	0	0	0
Ti	0	0	0	0	0	0	0	0
Fe	0.4	0.4	0.4	0.4	0.4	0.4	0.5	0.4
Mn	0	0	0	0	0	0	0	0
Mg	0.5	0.6	0.6	0.5	0.5	0.6	0.5	0.5
Ca	0.9	1	1	1	1	0.9	1	1
Na	0	0	0	0	0	0	0	0
K	0	0	0	0	0	0	0	0
Cr	0	0	0	0	0	0	0	0
P	0	0	0	0	0	0	0	0
Ba	0	0	0	0	0	0	0	0
XFe	0.23	0.21	0.21	0.21	0.22	0.2	0.24	0.22
XMg	0.27	0.29	0.29	0.29	0.28	0.31	0.26	0.29
XCa	0.5	0.5	0.5	0.5	0.5	0.5	0.5	0.5

Scapolite is a colourless non pleochroic which shows low relief and 1 set of cleavage with straight grain boundaries it shows high order interference colour. lamellar twinning is shown by the mineral grains another accessory mineral in this zone are Epidote crystal with moderate relief non pleochroic and 2nd order interference colour showing two orientation by the minerals. Spene and Apatite are other accessory minerals

Table No 4.3: Mineral chemistry and Structural Formulae of scapolite based on 12 oxygen

SiO ₂	46.2	43.38	46.11	45.92	46.32	46.17	45.75	46.32
Al ₂ O ₃	27.52	25.11	27.26	27.33	27.15	27.13	27.44	27.4
TiO ₂	0.04	0	0	0	0	0	0.06	0
FeO	0.07	0.05	0.07	0.19	0.13	0.07	0.15	0.09
MnO	0.03	0	0	0	0	0	0	0
MgO	0	0	0	0	0.02	0.01	0.02	0
CaO	17.96	22.55	18.44	18.18	18.32	18.07	18.54	18.27
Na ₂ O	3.45	1.96	3.3	3.53	3.41	3.42	3.39	3.46
K ₂ O	0.12	0.17	0.1	0.17	0.15	0.13	0.11	0.13
Cr ₂ O ₃	0	0	0.01	0	0.02	0	0	0
P ₂ O ₅	0.02	0.02	0	0.01	0.03	0.02	0.03	0
BaO	0	0.01	0	0	0	0	0	0.1
Ions								
Si	6.8	6.6	6.8	6.7	6.8	6.8	6.7	6.8
Al	4.8	4.5	4.7	4.7	4.7	4.7	4.7	4.7
Ti	0	0	0	0	0	0	0	0
Fe	0	0	0	0	0	0	0	0
Mn	0	0	0	0	0	0	0	0
Mg	0	0	0	0	0	0	0	0
Ca	2.8	3.7	2.9	2.9	2.9	2.8	2.9	2.9
Na	1	0.6	0.9	1	1	1	1	1
K	0	0	0	0	0	0	0	0
Cr	0	0	0	0	0	0	0	0
P	0	0	0	0	0	0	0	0
Ba	0	0	0	0	0	0	0	0
XCa	0.74	0.86	0.75	0.73	0.74	0.74	0.75	0.74
XNa	0.26	0.13	0.24	0.26	0.25	0.25	0.25	0.25
XK	0.26	0.13	0.24	0.26	0.25	0.25	0.25	0.25

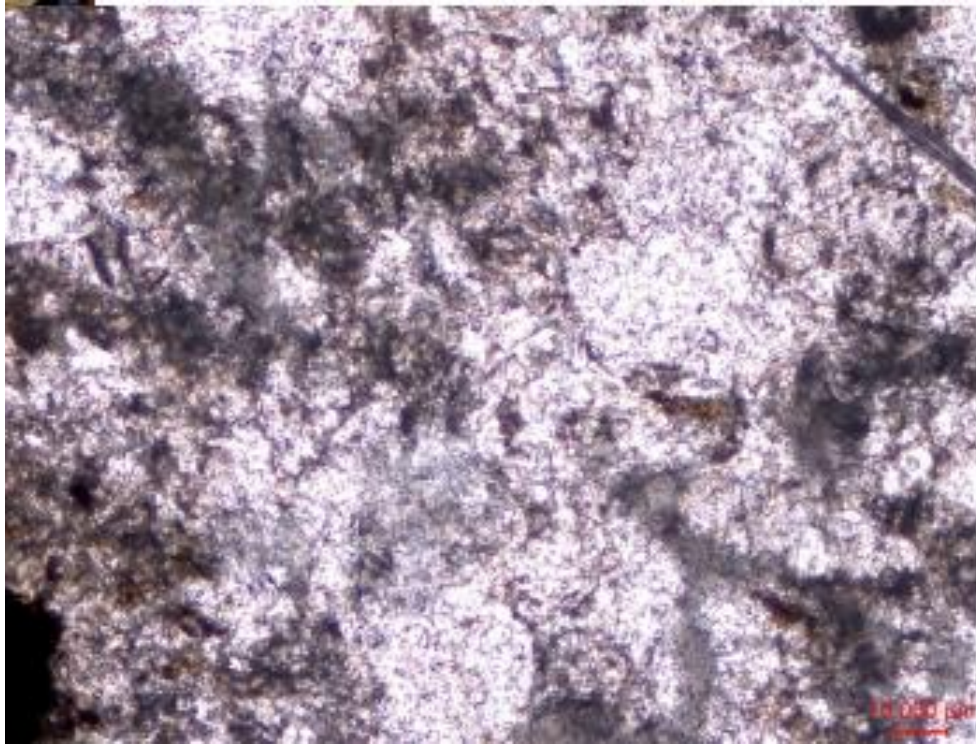


Figure 4.5 -Plane polarized photomicrograph showing grains of calcite and apatite surrounded by a cloudy matrix

Considering the orientation and occurrence of minerals in this layer is periodic. Within this layer where the Skeletal garnets are present they are associated with diopside ,Also zones of scapolite , calcite and a cloudy ground mass are present together. All the mineral show alignment horizontally are laterally this are intruded by shear, which is penetrative through garnets, calcite & pyroxene.

Quartz veins commonly crystallizes along this shears, Subgrains have a straight grain boundary, due to increase in strain, large quartz grains have formed subgrains indicated by the change in extinction angle of the adjacent grains having slightly developed grain boundary between the subgrain. grain thickening has occurred along the grain boundaries of the mineral.

Layer b

Second layer which makes major part of the sample is dominant in biotite, hornblende, diopside, quartz, k feldspar, ilmanite & Epidote. This mineralogy is present in a form of layered domains with the shear cross cutting the mineralogy. The green mineralogy separating the two layers is hornblende and Clino pyroxene.

Hornblende typically appears dark green to black in thin section. Hornblende crystals often display elongated prismatic or acicular shapes. The crystals may exhibit cleavage planes and are typically elongated parallel to the c-axis. Hornblende typically shows two well-developed cleavage planes intersecting at approximately 56 and 124 degrees. These cleavages are often visible in thin section and can help in identifying the mineral. Hornblende typically exhibits moderate to high birefringence under cross-polarized light. The grain size varies from medium to coarse. Orientation of this acicular grains is parallel to the foliation. From the hornblende domain entering the diopside domain, diopside grains ground the hornblende forming a mono mineralic corona texture. As we enter into the pyroxene domain the hornblende grain size will reduce and number of inclusion increases. (fig-4.5)

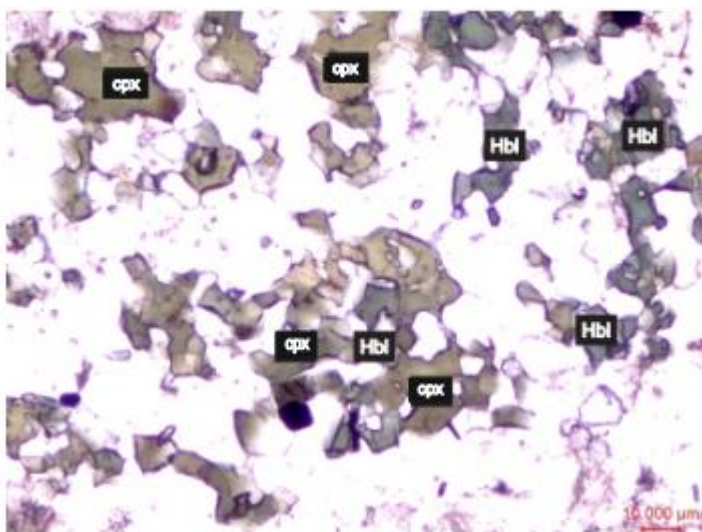


Figure 4.6-Plane polarized photomicrograph showing grains of hornblende surrounded by diopside.

The second domain is dominated by diopside having similar composition to the pyroxene in the white layer. Diopside commonly forms elongated prismatic crystals with well-defined cleavage planes. In thin section, these crystals may exhibit various forms depending on the specific conditions under which they formed. These grains have inclusion of apatite. Pyroxene domain is often includes skeletal garnets this garnets have similar characters compared to the garnets in the other band but compositionally this are rich in Fe.

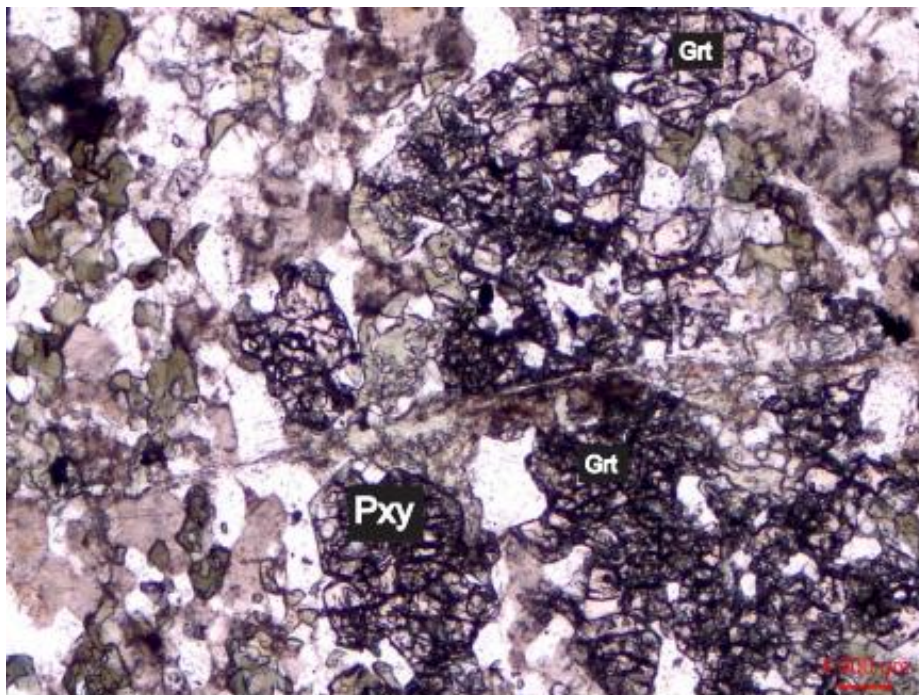


Figure 4.7-Plane polarized photomicrograph showing grains of diopside wrapping around skeletal garnets..

The third domain is characterized by biotite. Biotites, a phyllo silicate mineral with a flexible layering of silica tetrahedra and aluminium-oxygen octahedral, can deform plastically under high pressures and temperatures and are particularly well suited to form foliations. These biotites show lepidoblastic texture are used to identify the

direction and intensity of deformation. The flaky biotite grains showing pleochroism from light yellow to brown and straight extinction. The original fabric will curve in the new fabric which can be seen with the orientation of the biotite grains. The shape of biotites varies from subhedral to euhedral. The biotite flakes occupy the fractures and also beards of biotite wrap around the garnet grains. Biotite grains show two preferential orientation. Composition of the mineral is mentioned in table number 4. mica can be crystallize within the fractures making the orientation of the fracture. Biotite forms selvages around the Garnet porphyroclast. Garnets within this domain are euhedral in shape, elongated and fractured. (fig 2c)

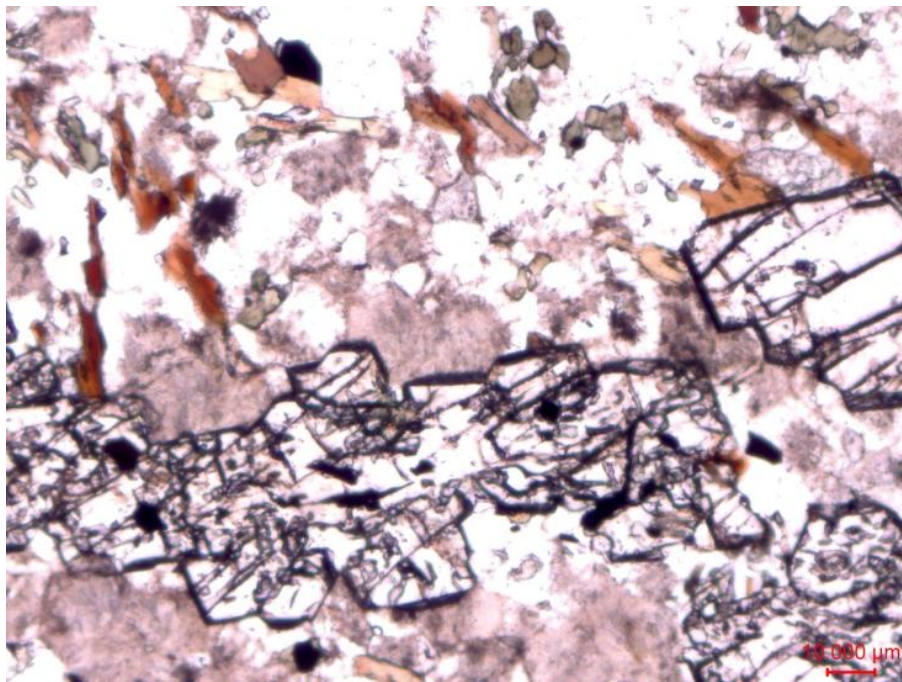


Figure 4.8-Plane polarized photomicrograph of garnet in the biotite domain

Table No 4.4: Mineral chemistry and Structural Formulae of Biotite based on 11 oxygen

oxides	Bt	Bt	Bt	Bt	Bt	Bt
	45	46	49	58	59	60
SiO ₂	36.53	36.43	36.53	36.46	36.15	36.43
Al ₂ O ₃	15.39	15.52	15.49	15.49	15.65	15.54
TiO ₂	3.07	3.17	3.08	2.79	2.81	2.87
FeO	19.84	19.61	20.25	19.47	19.2	20.02
MnO	0.03	0	0.03	0.05	0.01	0.04
MgO	10.23	10.28	10.14	10.22	10.19	10.39
CaO	0.01	0	0	0	0	0
Na ₂ O	0.17	0.21	0.26	0.2	0.22	0.15
K ₂ O	8.8	8.95	8.9	9.1	8.92	9.05
Cr ₂ O ₃	0.15	0.01	0.09	0.1	0.05	0.09
P ₂ O ₅	0	0	0.03	0	0	0
BaO	0.35	0.48	0.42	0.3	0.32	0.36
Calculated for 11 oxygen						
Ions						
Si	2.8	2.8	2.8	2.8	2.8	2.8
Al	1.4	1.4	1.4	1.4	1.4	1.4
Ti	0.2	0.2	0.2	0.2	0.2	0.2
Fe	1.3	1.3	1.3	1.3	1.2	1.3
Mn	0	0	0	0	0	0
Mg	1.2	1.2	1.2	1.2	1.2	1.2
Ca	0	0	0	0	0	0
Na	0	0	0	0	0	0
K	0.9	0.9	0.9	0.9	0.9	0.9
Cr	0	0	0	0	0	0
P	0	0	0	0	0	0
Ba	0	0	0	0	0	0
Si	2.8	2.8	2.8	2.8	2.8	2.8
Al <u>IV</u>	1.2	1.2	1.2	1.2	1.2	1.2
Al <u>VI</u>	0.2	0.2	0.2	0.2	0.2	0.2
XFe	0.5	0.5	0.5	0.5	0.5	0.5
XMg	0.5	0.5	0.5	0.5	0.5	0.5

Observing the sample laterally the grain size of biotite reduces and these grains have inclusions of hornblende. The porphyroclasts of hornblende are oriented parallel to the biotite grains but some grains orient themselves at an angle to the foliation.

Other mineralogy which characterizes this zone is Quartz. Quartz is colorless in plane polarized light with low relief and shows grey to yellow 1st order interference colors and has undulose extinction in BxP. The grains are subhedral to anhedral and most grains have a sinusoidal grain boundary with a few grains having straight boundaries. Due to an increase in strain, large quartz grains have formed subgrains indicated by the change in extinction angle of the adjacent grains having slightly developed grain boundaries between the subgrains. Quartz grains show grain boundary bulging. Along the shear quartz grains show an angular nature indicating that the zone has undergone brittle deformation. Quartz grains have formed subgrains and subgrain rotation has also occurred. Grain boundary sliding followed by formation of triple junctions between adjacent grains is also observed.

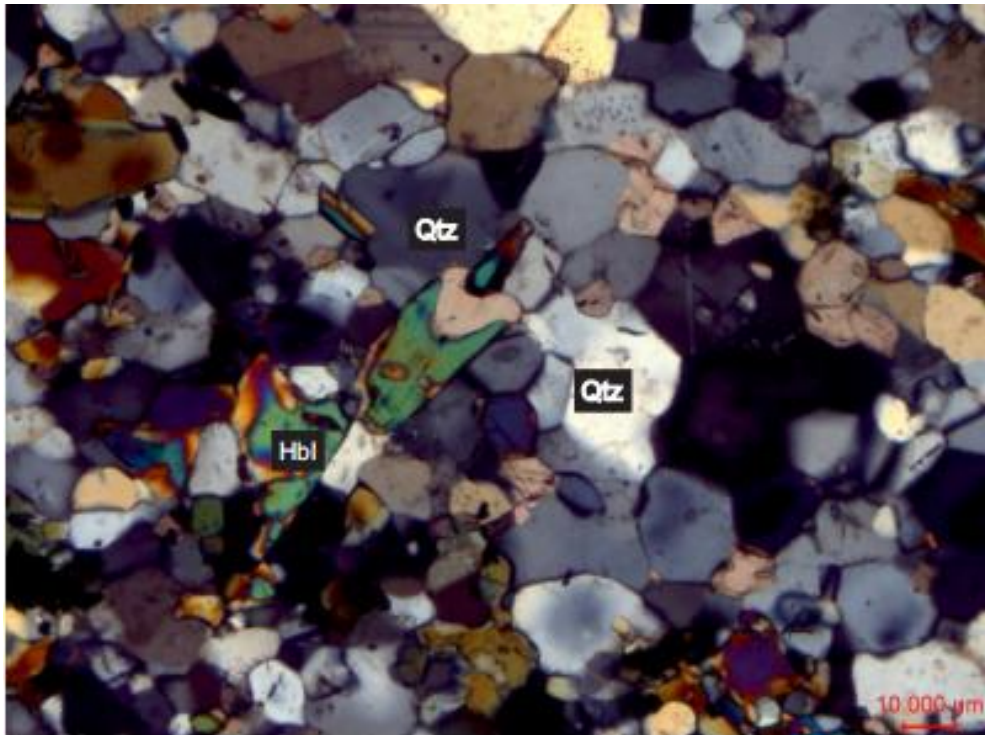


Figure 4.9-Cross polarized photomicrograph of Quartz showing bulging & straight grain boundaries

Plagioclase grains are sparsely present within the matrix. It is colorless and has low to moderate relief. It exhibits 1st order gray interference colors. Multiple lamellar twinning is also observed in these grains. Plagioclase grains in this layer are Na & Ca rich and plots in the Andesite & Labdorite zone of the Feldspar ternary plot. Some grains of plagioclase are showing sliding along the cleavage plane.

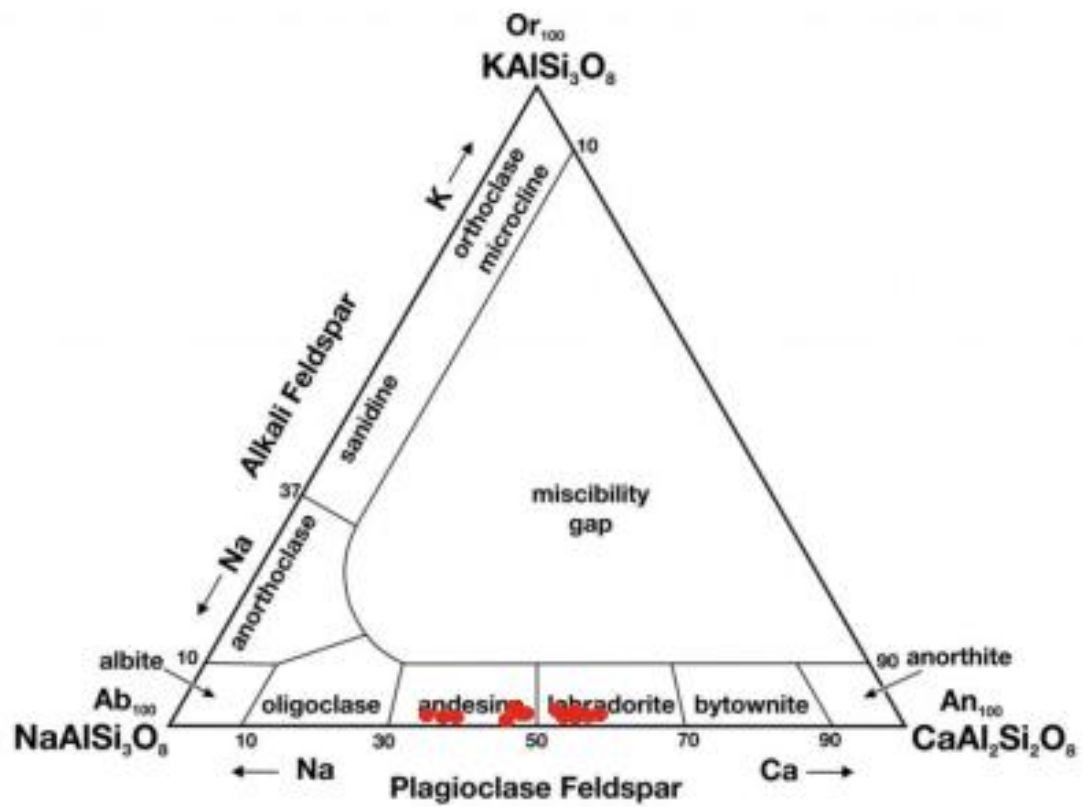


Figure 4.10- Tertiary plot for Feldspars.

Table No 4.4:Mineral chemistry and Structural Formulae of Orthoclase based on 8 oxygen..

oxides	Plg								
	14	15	16	17	74	75	76	77	78
SiO ₂	59.99	56.35	56.9	59.83	55.99	59.46	57.81	58.5	57.9
Al ₂ O ₃	25.23	28.04	27.75	25.78	27.66	25.68	26.47	26.34	26.66
TiO ₂	0.01	0.02	0	0	0.02	0.02	0	0	0.02
FeO	0.05	0.02	0.07	0.07	0.06	0.03	0.05	0.13	0.01
MnO	0.05	0	0.02	0.04	0	0.02	0	0.03	0
MgO	0.01	0	0	0.01	0	0.01	0.01	0	0.01
CaO	7.23	10.32	9.89	7.6	9.77	7.48	8.66	8.19	8.69
Na ₂ O	8.01	6.17	6.31	7.77	6.32	7.72	6.87	7.28	6.89
K ₂ O	0.11	0.04	0.1	0.09	0.09	0.12	0.11	0.16	0.13
Cr ₂ O ₃	0	0	0	0	0	0	0	0	0.02
P ₂ O ₅	0	0	0	0	0.02	0.03	0	0	0.01
BaO	0	0.01	0	0.04	0	0.01	0	0.03	0
Calculated for 8 Oxygen									
Ions									
Si	2.66	2.51	2.53	2.64	2.52	2.64	2.59	2.59	2.62
Al	1.32	1.47	1.46	1.34	1.47	1.35	1.4	1.4	1.37
Ti	0	0	0	0	0	0	0	0	0
Fe	0	0	0	0	0	0	0	0	0
Mn	0	0	0	0	0	0	0	0	0
Mg	0	0	0	0	0	0	0	0	0
Ca	0.34	0.49	0.47	0.36	0.47	0.36	0.42	0.42	0.38
Na	0.69	0.53	0.54	0.67	0.55	0.67	0.6	0.6	0.64
K	0.01	0	0.01	0.01	0.01	0.01	0.01	0.01	0.01
Cr	0	0	0	0	0	0	0	0	0
P	0	0	0	0	0	0	0	0	0
Ba	0	0	0	0	0	0	0	0	0
XCa	0.33	0.48	0.46	0.35	0.46	0.35	0.41	0.41	0.37
XNa	0.66	0.52	0.53	0.65	0.54	0.65	0.59	0.58	0.62
XK	0.01	0	0.01	0	0.01	0.01	0.01	0.01	0.01

K-feldspar shows a pitted appearance having low relief in plane polarized light. Under crossed polars feldspar grains show 1st order gray birefringence colors and have straight extinction. These grains have a sinusoidal grain boundary and have undergone the process of saussuritization and have formed clay minerals in some spots. along the shear the saussuritization is very high. may be due to the recent weathering of the rock.

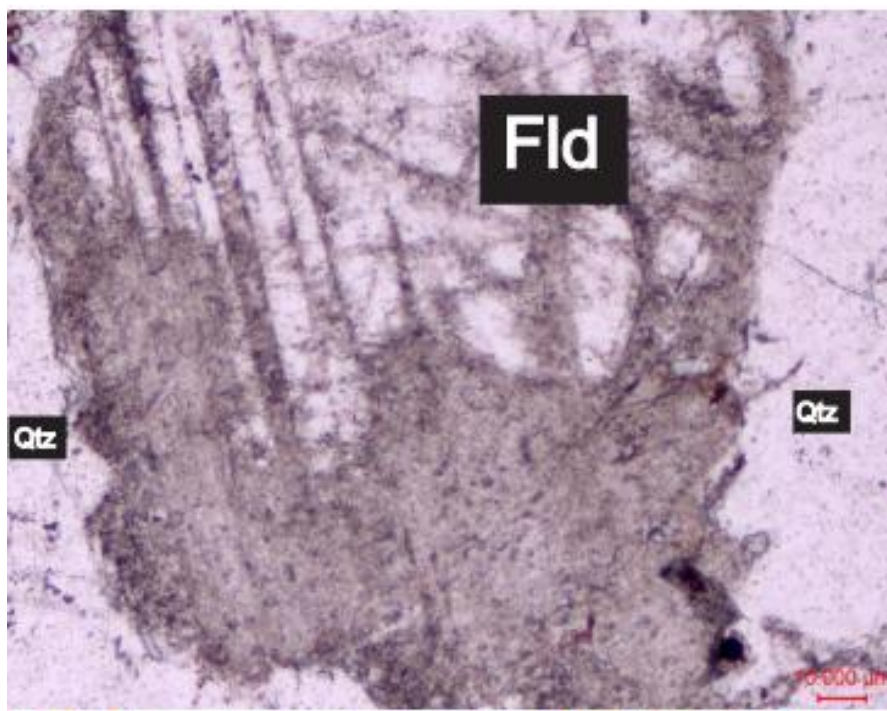


Figure.4.11-Plane polarized photomicrograph of saussuritization K feldspar along the shear

The shears deforms the minerals brittle or ductile based on the minerals present in the domain and also the orientation of minerals. there are Four major sets of shears within the sample .The vertical shear is formed due to tension forces characterized by

Quartz vein and Psudotechalite (Fig 3 a).The horizontal Shear (yellow colour) is characterized by Hornblende,Epidote ,Pyroxene Or Biotite.This shear is formed later than the tension as there is some displacement of the quartz vein.The conjugate shear (orange band) is only restricted to the (B) characterized by biotite.The slip shear (Blue Band) this shear extends throughout the specimen.Along this shear

In the Hornblend Quartz domains where hornblende is bounded by thin quartz layers, grain size reduction of hornblende is more pronounced .Hornblende is granulated to the smallest sizes along shear bands where cataclastic flow has occurred . In the middle of the Hornblend Quartz domains, the angle is minimal and the strung-out hornblende fragments are aligned subparallel fabric in the plastic quartz .similar situation is observed for Biotite & Quartz domain ,Garnet and Biotite domain where Garnet highly is granulated. The shear fracture have provided site for crystallization of secondary minerals , also as the composition of the rock varies there are different minerals formed along the shears.Oriented crystallized veins might have formed during the escape of fluids from the pelitic protolith during thy formation of the rock .Feldspar in the layer is highly saussuritized fig 4.11.

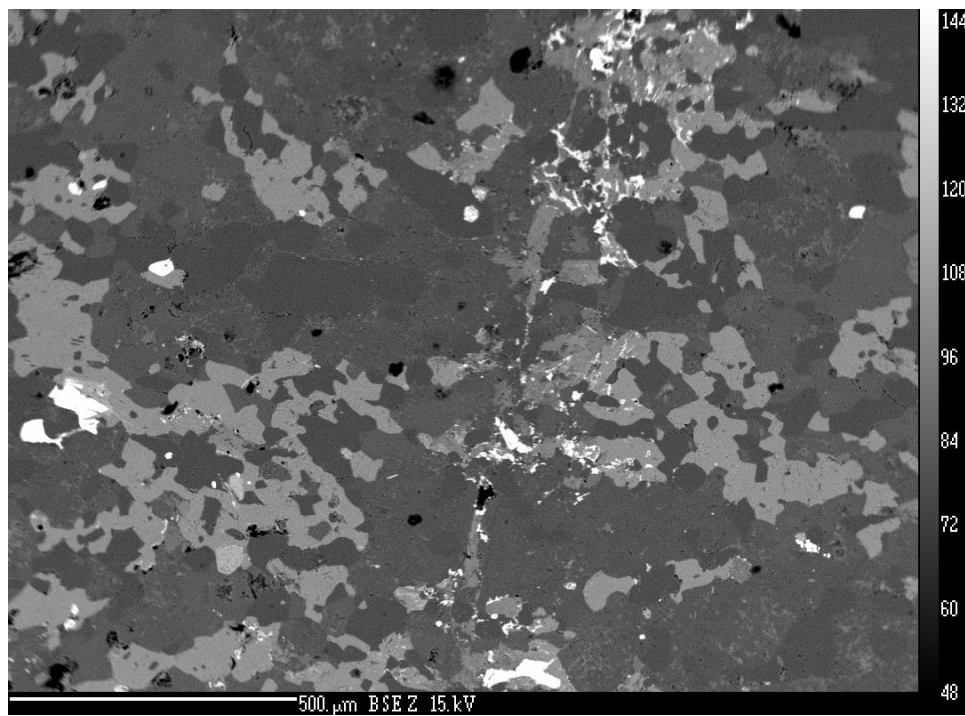


Figure 4.12: BSE images showing secondary precipitation of iron oxides along the shear planes

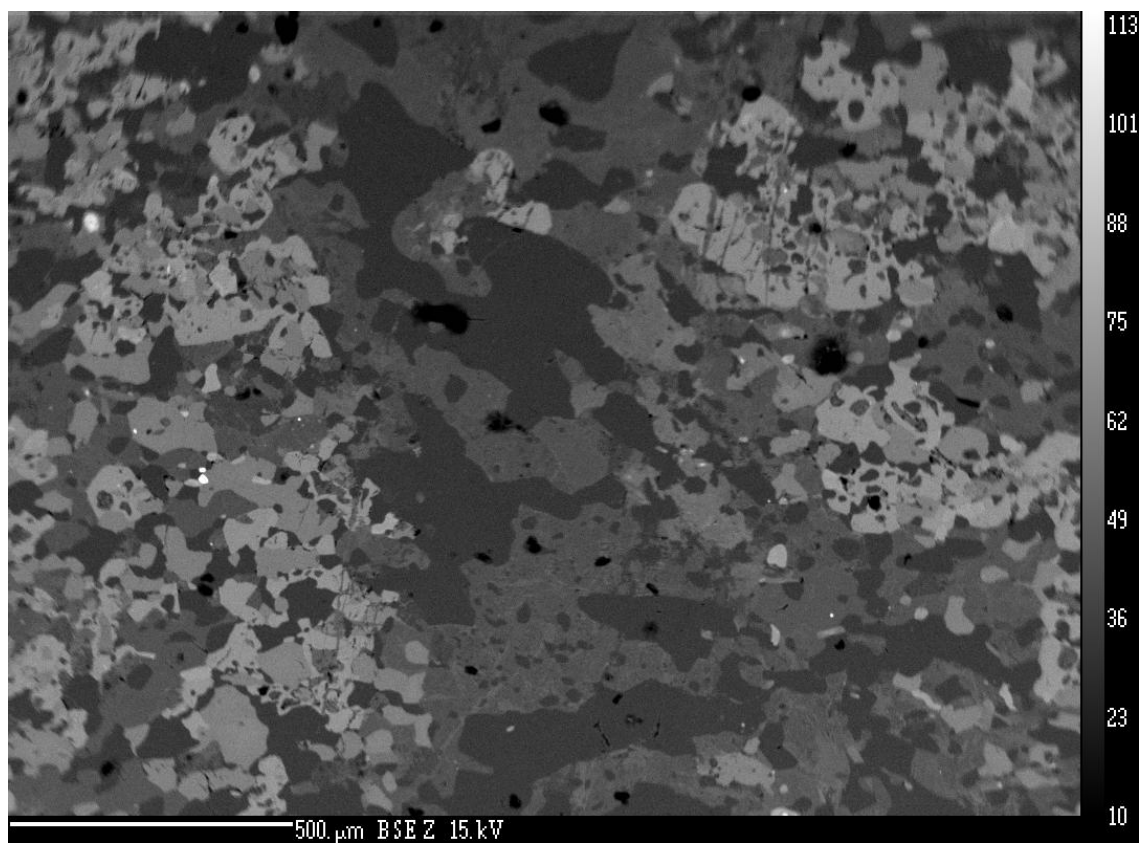


Figure 4.13: BSE images showing secondary precipitation along the shear planes

CHAPTER V :THERMOBAROMETRY

Table 5.1-Temperature (°C) at 7.5kbar conditions of calcic layer using conventional thermobarometers.

Temperature (°C) at 7.5kbar						
	Garnet -Biotite		Grt-Hbl		Hbl-Pl	Grt -Cpx
	1	2	3	4	5	6
Calcic layering /a	-	-	855°C	856°C	847°C	901°C
Matrix layer b1	597°C	592°C	523.°C	557°C	-	-
Matrix layer b2			554°C	475°C	561°C	576°C
Matrix layer b3	-	-	-	-	544°C	-

1)&2)Bhattacharya et al. (1992) using mixing parameters GS-Ganguly and Saxena (1984), HW-Hackler and Wood (1989): 3) Dasgupta et al.(1991): 4)Ferry and Spear (1978)5) Holland & Blundy (1994)6)Nakamura(2009).

Table 5.2-Pressure (Kbr) at 600°C conditions of calcic layer using conventional thermobarometers.

Pressure at 600°C				
	Hbl-Pl		GHPQ	Grt- Cpx- Pl(Qtz)
	7	8	9	10
Calcic layering /a	7.082Kbr	6.45Kbr	5.659Kbr	6.309kbr
Matrix layer b1			7.562kbr	
Matrix layer b2		6.652kbr		6.488 Kbr
Matrix layer b3	7.605Kbr	7.605Kbr		

7) Bhadra & Bhattacharya(2007):8)Molina et al.(2015):9)kohn & spear(1989):10)Eckert, newton & kleppa (1991).

Temperatures were estimated from Garnet-Biotite pairs using the thermometric formulations proposed byBhattacharya et al. (1992) using mixing parameters GS-Ganguly and Saxena (1984), HW-Hackler and Wood (1989): provided temperature changes for Garnet -Biotite pair in the rock specimen.Garnet-Hornblende

thermometer formulations by Dasgupta et al.(1991): Ferry and Spear (1978)5) Holland & Blundy (1994)6) Nakamura(2009). and Garnet - Clinopyroxene thermometric formulations proposed by Nakamura(2009).were used to understand the thermometry of the rock.For The Barometric study of the specimen Bhadra & Bhattacharya(2007) & Molina et al.(2015) praposed a barometer using Hornblende-Plagioclase ,A barometer praposed by kohn & spear(1989)Garnet-Hornblende-Plagioclase-Quartz (GHPQ) and Garnet-Clinopyroxene-Plagioclase-Quartz formulation by Eckert, newton & kleppa (1991).

Previous studies on the multiplayer garnet bearing schist expressed temperature ranges from 547°C -655°C for garnet-biotite pairs (Prahraj et al.2023) which matches with the temperature ranges acquired from various thermometric formulations .The calcic band layer shows an exeptionally higher temperature range for Dasgupta et al.(1991): Ferry and Spear (1978) Holland & Blundy (1994) Nakamura(2009).The temperatures ranges from 855°C -951°C. Dasgupta et al.(1991) provided a lower temperature of 475°C for the matrix.The multi layer matrix with Garnet-Hornblende & Biotite showed that the thermometers provided temperatures ranging from 597°C - 557°C for matrix.where as the second layer with the matrixdominated by Garnet-Hornblende - Clinopyroxene thermometer showed temperature variation from 554°C to 576°C & the last layer which is dominated by Hornblende ,Plagioclase & Quartz provided temperature of 554°C.

Pressures estimated using Hornblende-Plagioclase barometric formulation by Bhadra & Bhattacharya(2007)calculated pressure variation of 7.6-5.6kbar. The calcic layer pressure range varied from 7.6-5Kbar which is almost similar to the pressure range experienced by the over all litholgy .

The minerals show overgrowth and inclusion of other mineral ,grain boundary dissolution,this indicates that the minerals are not in equilibrium, therefore the thermometric & barometric data cannot be considered for these rocks.

CHAPTER VI : DISSCUSSION AND CONCLUSION

The garnetiferous biotite schists in around Sawantwadi in Sindhudurg have experienced several cycles of deformation (Rekha and Bhattacharya, 2014), that has resulted in several successive ductile foliations in the rocks. The present study for the first time describes the brittle deformation structures in the area. The most dominant brittle structures are cohesive cataclastic shears that occur as various cross-cutting sets in the outcrop and stand out because of differential weathering. In locations where the schists contain interbanded calc-silicate layers which are also more resistant to weathering, segregation of the cataclastic shears and the calc-silicate layers must be done carefully. Five major orientations of the cataclastic shears are reported in this area in this study (fig 3.4 & 3.5). Although two dominant sets of cataclastic shears along the E-W and N-S foliations are present, it does not indicate that brittle shearing was contemporaneous with the formation of the ductile foliation in the rocks. The foliation formation occurred at temperatures and pressures of 596°C and 7.6 Kbars as calculated from the geothermobarometry in the present work. The brittle shears occurred at much lower temperatures since chloritization and saussuritization is always associated with the fractures. Therefore it is apparent that the cataclastic shears possibly develop more easily along previously existing weaker foliation planes and the rheology of the rock plays a major part in controlling the extend of this features.

Thin section petrology of the shears shows angular fragments of quartz, grain sliding along the cleavages of hornblende and plagioclase, grain boundary dissolution, and locally pseudotachylite formation but the rock is still cohesive in nature indicating that although the rock has undergone brittle deformation, the deformation did not occur at the surface but rather at some depth within the crust. Along this fractures there is chloritization of minerals like biotite, garnet, clinopyroxene, hornblende and

epidote and secondary mineral precipitation of chlorite, iron oxides and occasionally calc-aluminum fibrous silicates. The occurrence of offsets along pseudotachylite veins and secondary mineralized zones indicate that there were at least two separate episodes of cataclastic shearing in the area.

In the field there are many shears exhibiting small displacements either sinistral, or dextral sense and rarely both shear senses along the length of the same shear. The dominant shears in the North-South foliated & ESE foliated outcrops are seen to generate two major sets of conjugate shears. Similar brittle structures are studied in the Navajo sandstones (Davis et al 1999) wherein the shears were related to Riedel Shear formation during the same episode of deformation. Comparing the brittle shears in Fig 1.3 to published and well accepted Riedel shear orientations, shows the orientation of the Principle Displacement zone / Shear zone (Fig. 6.1, 6.2).

The cataclastic shears produced in outcrops with dominantly N-S striking steep foliation is shown in Fig. 4.1. It can be seen that a dextral sense observed on the N-S cataclastic shear (Fig. 3.7) can be related with the P shear in the Riedel shear diagram. R shear which is the first to form is related to the second most dominant cataclastic shear orientation, i.e. N35° which also shows a dextral sense. This would indicate that the principle displacement zone is in the NNE direction and dextral. Tensional T shears are also prominently developed but the antithetic P' and R' shears are weakly formed (Fig. 6.1).

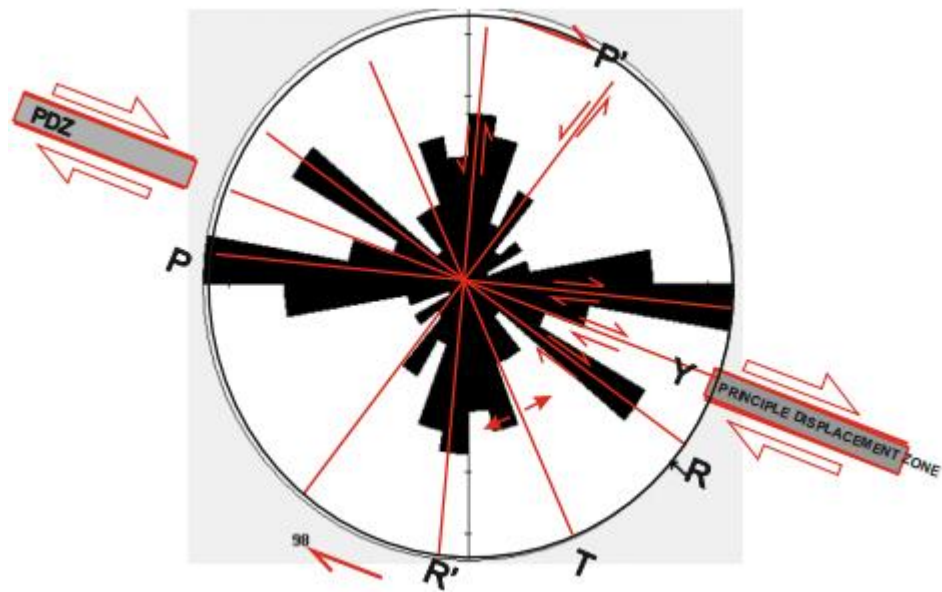


Figure 6.1: Correlating oriented shears of the N-S foliated outcrop with the Riedel shear diagram.

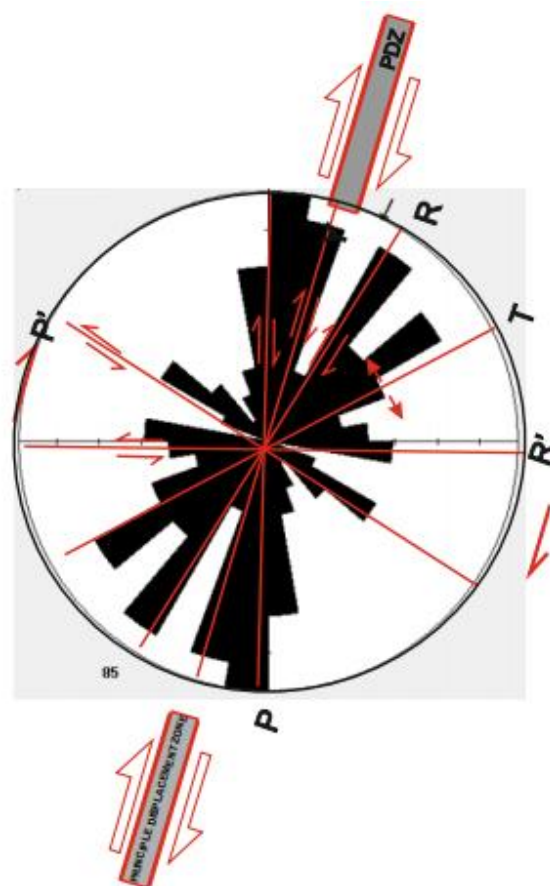


Figure 6.2: Correlating oriented shears of the ESE foliated outcrop with the Riedel shear diagram

The cataclastic shears produced in outcrops with dominantly ESE striking steep foliation is shown in Fig. 6.2. It can be seen that the synthetic P and R shears are again the most dominant shear set and form conjugate shears in field. The T shears are not very prominent but the R' shears are formed. This would indicate that the principle displacement zone is in the ESE direction and dextral (Fig. 6.2).

Both of the major brittle displacement zones in the Sawantwadi area of Sindhudurg trending NNE and ESE are thus orthogonal to each other.

Conclusion

In this study focusing on cataclastic shears, information was gathered and showcased through a structural map, revealing their structural influence. Further microscopic examinations revealed that these shears were formed through brittle processes, with secondary mineral deposition occurring along the fractures. The orientation of the shears was analyzed using the Riedel shear diagram, identifying brittle shear zones oriented in the NNE and ESE directions.

CHAPTER VII : REFERENCE

REFERENCES

- Anderson, J. L., Osborne, R. H., & Palmer, D. F. (1983). Cataclastic rocks of the San Gabriel fault—an expression of deformation at deeper crustal levels in the San Andreas fault zone. *Tectonophysics*, 98(3-4), 209-251.
- Babaie, H. A., & La Tour, T. E. (1994). Semibrittle and cataclastic deformation of hornblende-quartz rocks in a ductile shear zone. *Tectonophysics*, 229(1-2), 19-30.
- Barahate V.S., Shende K.P., 2018, Specialised thematic mapping of Precambrian rocks in Kundawadi- Dukanwadi-Pipalwadi- Talkat- Asaniya areas of Sindhudurg district, Maharashtra., GSI Open file report.
- Best. M.G., 2003. *Igneous and Metamorphic Petrology*, 2nd Edition, Blackwell publishing. ISBN: 978-1-405-10588-0
- Blenkinsop, T. G., & Rutter, E. H. (1986). Cataclastic deformation of quartzite in the Moine thrust zone. *Journal of Structural Geology*, 8(6), 669-681.
- Chadwick, B., Ramakrishnan, M., Viswanatha, M. N., 1981. The stratigraphy and structure of Chitradurga region: An illustration of cover basement interaction in the late archean evolution of the Karnataka craton, Southern India. *Precambrian Research* 16, p.31-54. [doi.org/10.1016/0301-9268\(81\)90004-8](https://doi.org/10.1016/0301-9268(81)90004-8)
- Chetty, T. R. K. (2023). Discovery of a Cataclastic Shear Zone from the East Dharwar Craton, India. *Journal of the Geological Society of India*, 99(11), 1508-1510.
- Chadwick, B., Vasudev, V.N., Hegde, G.V., 2000. The Dharwar craton, southern India, interpreted as the result of late Archean oblique convergence. *Precambrian Research* 99, p. 91-111. doi:10.1016/s0301-9268(99)00055-8
- Dashputre A.S., Jadhav P.B., Marathe T., 2019. Microstructural evolution of the garnet metapellites near Sawantwadi, Sindhudurg District, Maharashtra. *Himalayan Geology*. Vol. 40 (1), 2019, pp. 58-66.
- Deshpande, G.G., Pitale U.L. 2014. *Geology of Maharashtra (2nd Edition Revised)*. Geological Society of India 266p. ISBN No: 978-93-80998-00-8.
- Foote, R.B. Geological features of the south Maharatta country and adjoining districts. 1876. *Memoir of the Geological Survey of India*, 12(2), 70-133.
- Fossen H., *Structural Geology*, 2010. Cambridge University Press, ISBN-13 978-0-521-51664-8.
- Fossen, H., & Cavalcante, G. C. G. (2017). Shear zones—A review. *Earth-Science Reviews*, 171, 434-455.

Ghodke S.S. A reappraisal of stratigraphy and structure of Dharwar Supergroup of the rocks of Sindhudurg district, Maharashtra. 1983. In Phadke A.V., Phansalkar V.G. (eds.), Prof. Kelkar Memorial Volume, Ind. Soc. Earth Science, 25-2.

Ghodke, S.S, Raghunathan V.A. 1970. GSI Field Season Report. FS 1969-1970, Geology of parts of Sawantvadi Taluka, District Ratnagiri, in topo-sheet no. 48 e/13.550.8(547.1) RAT: 526p.

Gupta, N., Jayananda, M., & Tandon, S. K., Geodynamics of the Indian Plate, 2020. Springer Geology. doi:10.1007/978-3-030-15989-4.

Higgins, M. W. (1971). *Cataclastic rocks* (No. 687). US Govt. Print. Off.,.

Hokada T., Horie. K., Kumar. M.S., Ueno. Y., Nasheeth. A., Mishima K., Shiraishi K., An appraisal of Archaean supracrustal sequences in Chitradurga Schist Belt, Western Dharwar Craton, Southern India. 2013. Precambrian Research, Volume 227, April 2013, Pages 99-119, doi.org/10.1016/j.precamres.2012.04.006.

Ishwar-Kumar, C., B. F. Windley, K. Horie, T. Kato, T. Hokada, T. Itaya, K. Yagi, C. Gouzu, and K. Sajejev. 2013, A Rodinian suture in western India: New insights on India Madagascar correlations, Precambrian Res., 236, 227-251. dx.doi.org/10.1016/j.precamres.2013.07.023.

Iyer, L.A.N. The geology of South Ratnagiri and parts of Sawantvadi State, Bombay Presidency. 1939. Records of the Geological Survey of India, 74, 504-529

Jayananda, M., Chardon, D., Chetty, T. R. K., Peucat, J.-J. Precambrian continental strain and shear zone patterns: South Indian case. 2008. Journal of Geophysical Research: Solid Earth, 113(B8). doi: 10.1029/2007jb005299.

Kelkar, K.V. 1956. On some Archean rocks in the southern parts of Ratnagiri district. Journal University of Poona, Science & Technology 10, 86-99.

Passchier, C. W., & Williams, P. R. (1996). Conflicting shear sense indicators in shear zones; the problem of non-ideal sections. *Journal of Structural Geology*, 18(10), 1281-1284.

Rekha, S., and A. Bhattacharya, Growth, preservation of Paleoproterozoic-shear-zone- hosted monazite, north of the Western Dharwar Craton (India), and implications for Gondwanaland assembly, (2013), Contrib. Mineral. Petrol., 166, 1203-1222. doi. 10.1007/s00410-013-0917-y.

Rekha, S., Bhattacharya, A. 2014. Paleo/Mesoproterozoic tectonism in the northern fringe of the Western Dharwar Craton (India): Its relevance to Gondwanaland and Columbia supercontinent reconstructions. American Geophysical Union, 33(4), 552-580. doi:10.1002/2013TC003335.

S. Rekha, T.A. Viswanath, A. Bhattacharya, N. Prabhakar. Meso/Neoproterozoic crustal domains along the north Konkan coast, western India: The Western Dharwar Craton

and the Antongil-Masora Block (NE Madagascar) connection. 2013. *Precambrian Research* 233 (2013) p.316-336, [dx.doi.org/10.1016/j.precamres.2013.05.008](https://doi.org/10.1016/j.precamres.2013.05.008).

Scrivener, K., Snellings, R., Lothenbach, B., & Press, C. R. C. (Eds.). (2016). *A practical guide to microstructural analysis of cementitious materials* (Vol. 540). Boca Raton, FL, USA.: Crc Press.

Spray J. G. 1997. Super faults; *Geology* (1997) vol-25: p.579-582. [doi.org/10.1130/0091-7613\(1997\)025-0579:S>2.3.CO;2](https://doi.org/10.1130/0091-7613(1997)025-0579:S>2.3.CO;2).

Spray J. G. 1998. Localized shock and friction-induced melting in response to hypervelocity impact. In: *Meteorites: Flux with time and impact effect*, Geological Society of London. pp. 171-180.

Swami Nath. J., Ramakrishnan, M. Viswanantha, M.N., 1976. Dharwar stratigraphic model and Karnataka craton evolution. *Records Geological survey of India* 107, p.149-175.

Swami Nath. J., Ramakrishnan, M., 1981. Early Precambrian suoracrustals of southern Karnataka. *Memoir Geological society of India* 112, p.350

Trouw R. A. J., Passchier. C. W., Wiersma. D.J., 2010. *Atlas of Mylonites- and related microstructures.*, Springer publication, doi.org/10.1007/978-3-642-03608-8.

Vernon. R.H., Clarke G.L., 2009. *Principles of Metamorphic Petrology*; Cambridge university press. ISBN 9780521871786.

Wilkinson, C.J. 1871. Sketch of geological structure of southern Konkan, *Records of the*

Winter J.D., *An Introduction to igneous and metamorphic petrology*. 2001. Prentice Hall publication, ISBN 0-13-240342-0 1. *Geological Survey of India*, 6, 44-47.

Woodcock, N., Schubert, C., 1994. Continental strike-slip tectonics. In: Hancock, P. (Ed.), *Continental deformation*. Pergamon Press, New York, pp. 251±263.